 doi:10.20944/preprints201810.0025.v1

# Modeling and Simulation of Fuzzy logic based Hybrid power for Electrification System in case of Ashuda Villages

*Abraham Hizkiel(Lecturer), Bahir Dar University institute of Technology (2018)*

*Email- hizkielabraham@yahoo.com*

Laksmi Gantasala(Lecturer) *), Debre Markos University institute of Technology (2018)*

*Email- glsrdmu@gmail.com*

## *ABSTRACT*

*Ethiopia is a developing country, where majority of the population lives in rural areas without access to electricity. 83% of the total population of the country use traditional biomass energy as a basic source of energy. In contrast, the country is endowed with sufficient renewable energy resources which can be used as a standalone electric energy supply system for electrifying remote areas of the country. These resources are mainly micro hydropower and wind which can be used individually or the best combination of one another. The application of hybrid renewable energy system has become an important alternative solution for rural electrification program.*

*The Modeling and control of a hybrid PV-Wind-Hydro DG system is also addressed. Dynamic models for the major system components, namely, wind energy conversion system, PV energy conversion system, hydro, inverter, and overall fuzzy logic controller units are developed. Then, a simulation model for the proposed hybrid power system has been developed using MATLAB /Simulink environment. This is done by creating subsystem sets of the major dynamic component models and then assembling into a single aggregate model. The overall power management strategy for coordinating and/or controlling the different energy sources is also presented in the thesis work. Generally there are 800 households with total electric demand of 71.6KW.To satisfy this demand 52%, 35% and 13% is to be contributed from wind/hydro/solar respectively. To use the power economically fuzzy logic controller is used. The controller monitors the demand and the available sources and then switches to the appropriate power supply according to the written rules. Simulations have been carried out to verify the system dynamic performance using a practical load profile and weather data. The result shows that the overall power management strategy is effective and the load demand is balanced. To complete this work, a grid extension from the closest substation has been compared with hybrid system. Cost of the grid extension is estimated based on the data obtained from EEP office. This is done in order to compare the cost of the designed hybrid power system against the cost of grid extension. The result shows that breakeven grid extension distance to be 23.9km which indicates that grid extension is preferable.*

***Key Words**: PV-Wind-Hydro Hybrid Power System, Dynamic Modeling, Load Profile, Grid Extension, smart micro grid, fuzzy logic controller, and mat lab/Simulink.*

 doi:10.20944/preprints201810.0025.v1

# 1. INTRODUCTION

There are no reasons that in the future our existence will be more and more dependent upon the energy. To satisfy their energy requirement, the people attention tends to electrical energy. Electrical energy is considered as superior to all other forms due to cheapness, convenient and efficient transformation, easy to control, cleanness, greater flexibility and versatile form. It finds innumerable uses in home, industry, agriculture, transport, defense, aviation, public center, etc. Electrical energy is not only for doing desired activities but also to improve quality of life of the people [1].

Among the very many important forms of energy available to any country, electrical energy is one important energy form that has contributed substantially to rapid economic growth and industrialization. The desirability and usefulness of electrical energy to the world cannot be over-emphasized. Electrical energy is useful in industrial, commercial and residential establishments. Electrical energy is useful in all manufacturing, telecommunications, residential (lighting, heating, cooling, entertainment) and commercial activities [2].

Electrical energy can be derived from diverse sources such as hydro (Electrical energy from water sources), nuclear, wind, solar (Energy from the sun) and the thermal sources. Therefore, the sources of electrical energy can be grouped into two main categories renewable and non-renewable sources. Renewable sources are sources of energy which can be recovered within one‘s life time (taken to be 70 years) [2].

## 1.2. Problem statement

Most of the remote rural areas of Ethiopia are not yet electrified. Electrifying the remote areas by extending grid system to these rural communities is difficult and not economical. As the current international trend in rural electrification is to utilize renewable energy resources; solar, wind, biomass, and micro hydro power systems can be seen as alternatives. Among these, wind, hydro and solar energy systems in stand-alone or hybrid forms are thought to be ideal solution for rural electrification due to abundant solar radiation and significant wind distribution availability nearby the rural community in Ethiopia.

Ethiopia is located in the eastern part of Africa between 3° to 15° north and 33° to 48° east, and thus the potential benefits of renewable energy resources such as solar and wind energy can be

Preprints (www.preprints.org) | NOT PEER-REVIEWED | Posted: 2 October 2018 doi:10.20944/preprints201810.0025.v1

considerable. The government of Ethiopia with the collaboration of Chinese government prepared solar and wind master plan for the whole country, which can be very useful to identify the gross amount distribution condition of solar and wind energy resource, construction conditions, cost and other limiting factor of wind and solar power generations [3].

Based on the analysis of this master plan:

- Ethiopia has a potential of 45,000MW of energy from hydro
- Ethiopia has a potential 1,350 of energy from wind
- Ethiopia has annual total energy of 2.199milion TWh/annum

So far, these vast renewable energy resources are not exploited sufficiently in the country, primarily due to the lack of scientific and methodological know how as regards planning, site selection, and technical implementation. A further constraint prohibiting their utilization is that the real potential of these resources is not well-known, partly because of the lack of research emphasis in developing these technologies.

Thus, in this thesis a hybrid renewable power generation system integrating these vast solar, hydro and wind resources is designed and modeled, to electrify the community living in Ashuda.

## 1.3. Objectives of the Study

### 1.3.1. General objective

The general objective of this study is to design, and model PV, hydro and Wind smart Micro -Grid Power generation system for hybrid electrification of remote villages in Ashuda.

### 1.3.2. Specific objectives

- To study the solar photovoltaic, hydro and wind energy potential of the study area.
- To estimate loads for specific village and nearby community.
- To design smart micro-Grid renewable energy system for the village.
- To simulate the system with HOMER and MATLAB or Proteus software
- To compare the investment cost of the hybrid system against the cost required to electrify the areas by extending the national grid.

## 2.1. Energy demand profile detail analysis

The first step in designing power system is determining the total power consumption of the study area. The size and cost of hybrid system components are highly influenced by the size of electrical loads. The necessary steps to estimate electricity required in the study area is to list all electrical

Preprints (www.preprints.org) | NOT PEER-REVIEWED | Posted: 2 October 2018 doi:10.20944/preprints201810.0025.v1

appliances, estimate its rating power , multiply by number of hours used in each day and add up the watt hours for all appliances.

Accordingly, Average load demand per hour is 71.1KW.

$$\text{Peak load} = \frac{Average\ load}{Load\ factor} \quad 2.1$$

LF is 0.072(given in homer), therefore peak load is 994KW

Installed capacity=peak load + loss (assume loss is 10% peak load, 99.4KW. installed capacity =Peak load + loss=99.4 +994=1093.4KW. Therefore the total electric energy demand of the village is 1093.4KW.

## 2.2. Wind system designing and sizing

The total electrical demand of the village is calculate as 71.6KW. In designing hybrid system 52 %( 37.2) is to be covered by wind power. The system loss is assumed 10%, therefore the installed capacity=37.2+37.2*0.1=40.9KW.

### 2.2.1. Wind Turbine Subsystem Model

The wind turbine is modeled by the power curve equation indicated in eq. (3.2).

$$\text{Pwind(t)} = \frac{1}{2}\text{PArotorV}(t)^3 Cp \quad 2.2$$

For the available temperature data:

$$\rho = \frac{\rho_0}{RT}\exp(-\frac{gz}{RT})[kg/m^3\ ] \quad 2.3$$

Where $\rho_o$ is standard sea level atmospheric pressure, g is gravitational constant (9.81m/s$^2$), and z is the region elevation (m) [34].

If pressure and temperature data is not available the formula in eq(3.3) is used for estimating the air density[34]

$$\text{P=1.225-(1.194*10^-4)*z}[kg/m^3 \quad 2.4$$

The air density (ρ) of the study area (Ashuda) is 1.147kg/m$^3$ (as it is calculated on the eq. (3.4). The rotor area of PGE 20/25 wind turbine is 305 m$^2$ [35]. Coefficient of power of a wind turbine (Cp) is taken as 59% = 0.59. The hub heights of PGE 20/25 wind turbine are 24/30/36 meter [35] and for this study, 36m is used. Gear and generator efficiency of 95 % is also considered (hence,

Preprints (www.preprints.org) | NOT PEER-REVIEWED | Posted: 2 October 2018 doi:10.20944/preprints201810.0025.v1

cumulative efficiency of gear-generator =0.95×0.95=90.25 %). With this detail's, the wind turbine in MATLAB/Simulink is given below in figure 2.1.

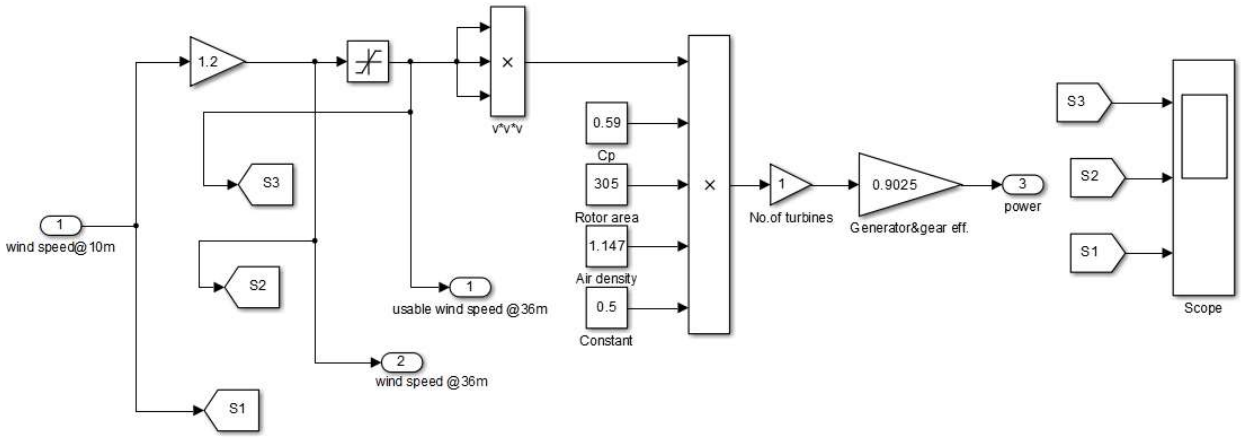


Figure 2.1: Expanded view of the wind turbine model

## 2.3. Photovoltaic system designing and sizing

The total electrical power demand of Ashuda village is 71.6KW. 13% of the total power demand is covered by, (0.13*71.6=9.3KW) solar pv system. Assume the system power loss is 10%, is 0.93KW. The total generation capacity of the pv system is 10.2KW. To calculate a number of parallel (Np), assume the system voltage is 12($V_m$), a string with four series (NS), the rated solar power is 135.

$$\mathrm{Np} = \frac{Peak\ power}{Rated\ powe * Ns} = \frac{10.2KW}{135 * 4} = 19 \qquad 2.5$$

Therefore, total number of modules of solar system, can be calculated as N=Ns*NP= 76 modules. Assume a single solar module having 0.4$m^2$cross sectional area ,the total area required for solar panel is can be calculated as follows AP=0.4*76=30.4$m^2$.

The size of the Inverter is determined by the AC load required with consideration for surge power. Inverter size should be 25-30% bigger than the total watts of the loads the specification inverter date obtained. Maximum AC load is 10.2kw, inverter constant is 1.25. Therefore Inverter rating is maximum AC x 1.25 = 27*1.25 = 12.75KW.

### 2.3.1. PV Subsystem Model

The equivalent circuit for the solar module arranged in NP parallel and NS series is shown in figure 3.2 below.

Preprints (www.preprints.org) | NOT PEER-REVIEWED | Posted: 2 October 2018 doi:10.20944/preprints201810.0025.v1

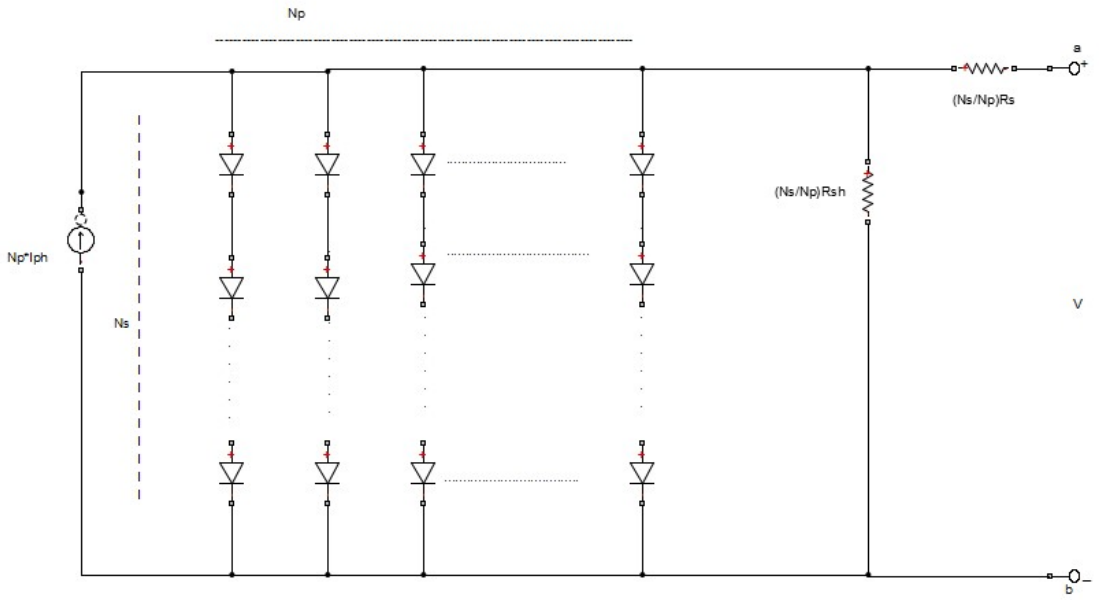


Figure 2.2: Circuit model of a generalized PV array [36]

The terminal equation for the current and voltage of the array becomes expressed in eq. (3.6) as stated in [34].

$$I = NpIph - NpIs\left(exp\left(\frac{q(\frac{V}{Ns}+\frac{IRs)}{Np}}{KTca}\right)-1\right)-\frac{\frac{NpV}{Ns}+IRs}{Rsh} \quad 2.6$$

Where: $I_{PH}$ is a light generated current or photocurrent, $I_S$ is the cell saturation of dark current, $q$ (= 1.6 ×10−19C) is an electron charge, $k$ (= 1.38 ×10−23J/K) is a Boltzmann's constant, $T_C$ is the cell's working temperature, $a$ is an ideal factor, $R$SH is a shunt resistance, and $R$S is a series resistance. The photocurrent mainly depends on the solar insolation and cell's working temperature, which is described as:

$$I_{PH} = (I_{SC} + K_1(T_c - T_{Ref}))^{\lambda} \quad 2.7$$

Where: $I_{SC}$ is the modules short-circuit current at a 25°C ($T_{Ref}$) and 1kW/m$^2$, $K_I$ is the cells short-circuit current temperature coefficient, $T_{Ref}$ is the cell's reference temperature, and λ is the solar insolation in kW/m$^2$.

$$T_C = T_{Air} + \frac{NOCT-20}{80}S \quad 2.8$$

Preprints (www.preprints.org) | NOT PEER-REVIEWED | Posted: 2 October 2018 doi:10.20944/preprints201810.0025.v1

S = insolation in MW/cm$^2$. (With $T_{Air}$ = 20.1 ºC, NOCT = 47.9 ºC and S =80 mW/cm$^2$), $T_c$ is calculated as 49.1 ºC. In order to know the values of Np and Ns, thesolar module has been selected. The specification of this module is found in the appendix A.

For a typical module cell, $R_S$ = 0.05 to 0.10 ohm and $R_{SH}$ = 200 to 300 ohms [37]. Therefore, for this study the average value of each, that is, RS = 0.075 and $R_{SH}$ = 250 is used.

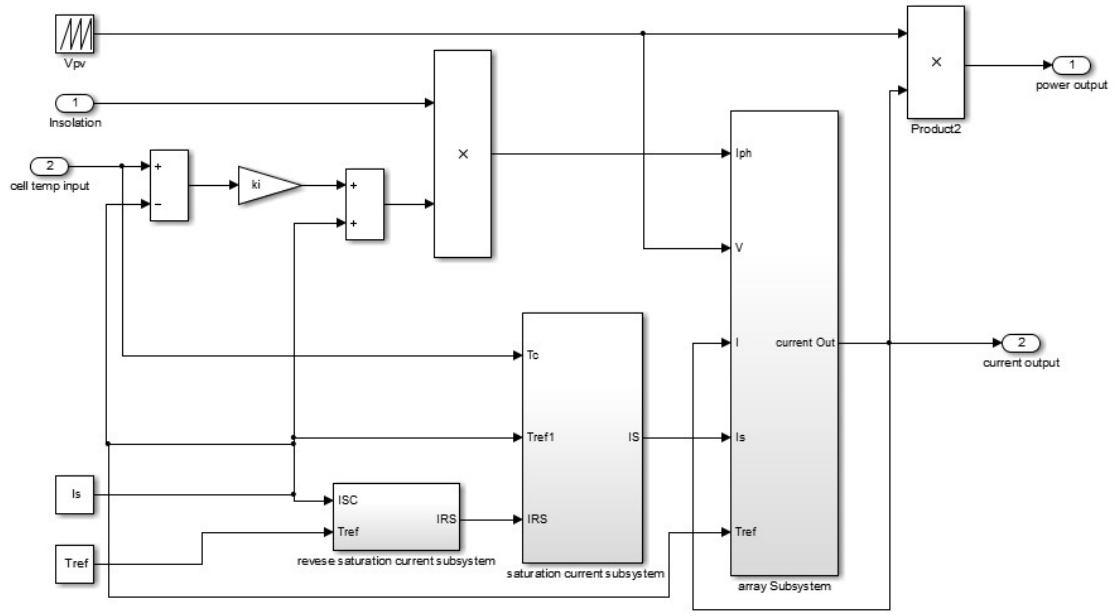


Figure 2.3: Model of PV modules

On the other hand, the cell's saturation current varies with the cell temperature, which is described as [34].

$$\mathrm{Is} = IRS\left(\frac{\mathrm{Tc}}{Tref}\right)^3 \exp\left[qEg\left(\frac{1}{Tref} + \frac{1)}{Ka}\right)\right] \qquad 2.9$$

Where: $I_{RS}$ is the cell's reverse saturation current at a reference temperature and a solar radiation and Eg is the band gap energy (an energy range in a solid where no electron states can exist and it is equal to 1.11 for Silicon semiconductor [38]) of the semiconductor used in the cell. The ideal factor *a* is dependent on PV technology and 1.3 is used for multi crystal solar module in this study from [34].

Preprints (www.preprints.org) | NOT PEER-REVIEWED | Posted: 2 October 2018 doi:10.20944/preprints201810.0025.v1

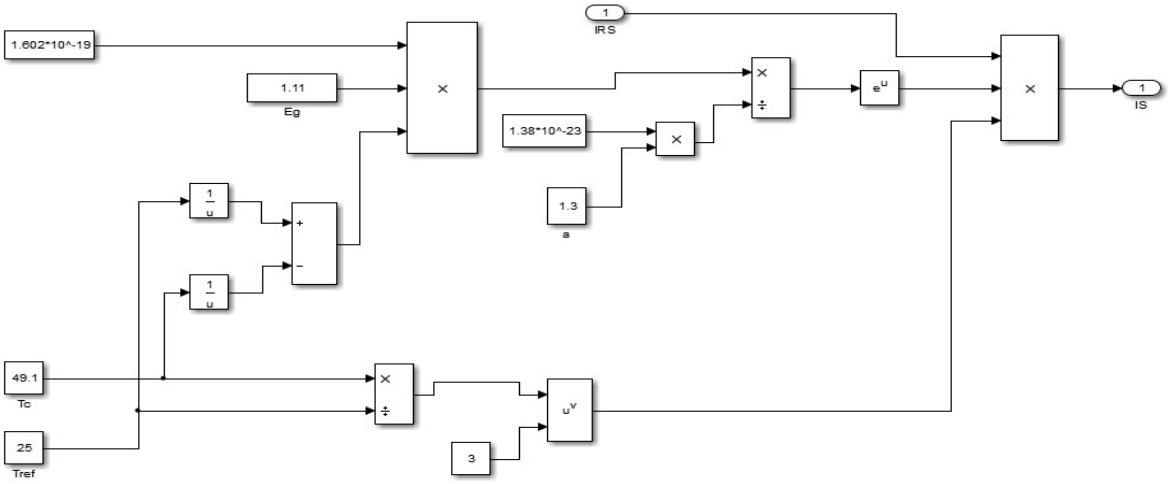


Figure 2.4: expanded view of saturation current subsystem

Given the PV open-circuit voltage, $V_{OC}$, at reference temperature and ignoring the shunt leakage current, the reverse saturation current at reference temperature can be approximately obtained as [36].

$$I_{RS} = \frac{Isc}{\left(\exp\left(\frac{qVoc}{NsKaTref}\right)-1\right)} \qquad 2.10$$

Preprints (www.preprints.org) | NOT PEER-REVIEWED | Posted: 2 October 2018 doi:10.20944/preprints201810.0025.v1

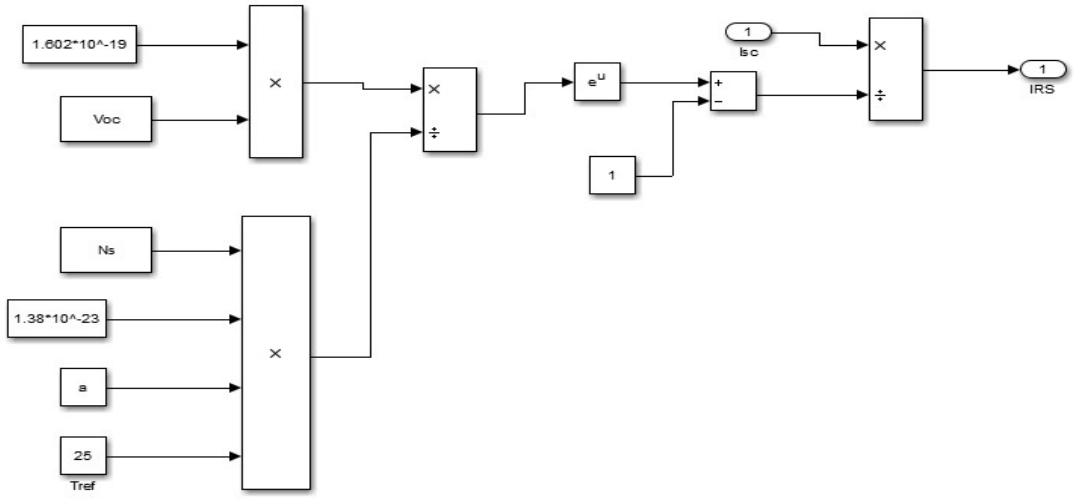


Figure 2.5: Expanded view of reverse saturation current mode

The detail of the array subsystem model in the Simulink is given in the figure 2.6.

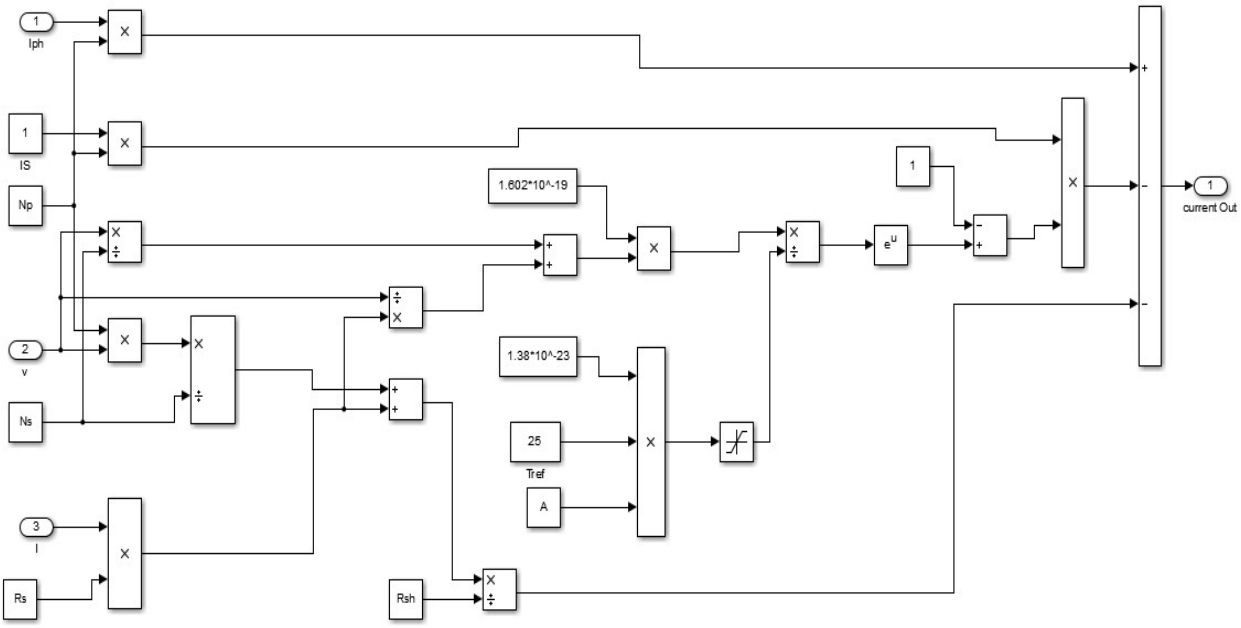


Figure 2.6: Expanded view of the array subsystem

For easy simulation, the solar radiation intensity for a sample day is assumed to be of a Gaussian function which is defined as [34]:

Preprints (www.preprints.org) | NOT PEER-REVIEWED | Posted: 2 October 2018 doi:10.20944/preprints201810.0025.v1

$$\Lambda(t)=\Lambda_{max}\exp[-(\frac{(t-tc)2}{2\sigma 2})] \qquad 3.11$$

Where: $\lambda_{max}$ is the maximal radiation intensity at a given time, $t_C$ is the center time, and σ is the standard deviation of Gaussian function. Figure 5.9 shows a plot of the Gaussian function for the solar radiation intensity of a sample day for different months generated from the given monthly average radiation data (in kWh/m$^2$/d) inputs by HOMER. As the figure clearly shows, the maximum average value of the Gaussian function is 0.8. Hence, with the conditions: $\lambda_{max}$ = 0.8kW/m$^2$, $t_c$ = 12, and σ = 2 a MATLAB/ Simulink model has been developed for simulation as indicated in figure 3.9. The output from this model is also indicated in figure 3.7and it is the same as HOMER estimates.

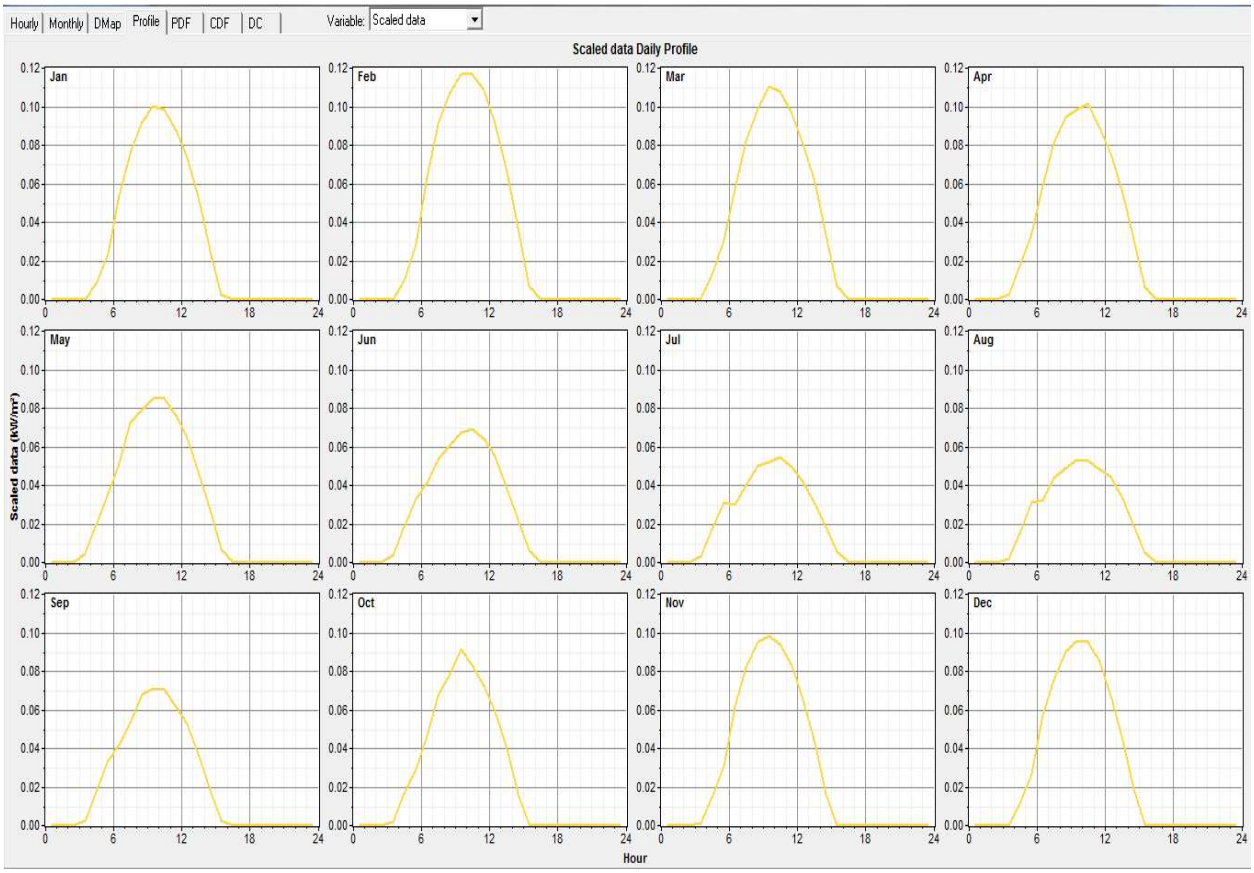

Preprints (www.preprints.org) | NOT PEER-REVIEWED | Posted: 2 October 2018 doi:10.20944/preprints201810.0025.v1

Figure 2.7: Scaled data solar insolation's in kW/m$^2$ in HOMER

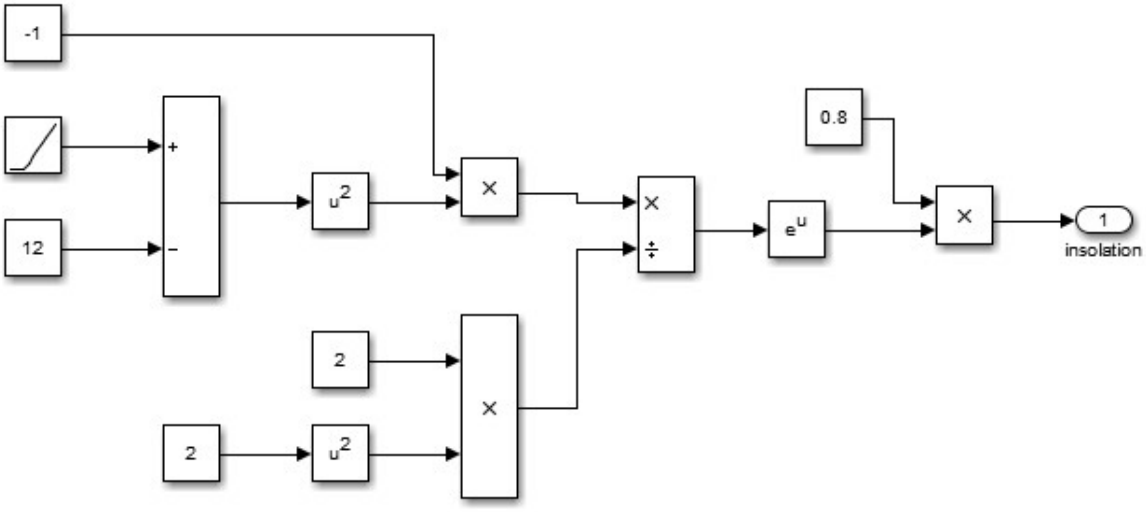


Figure 2.8: Expanded view of insolation subsystem model

Preprints (www.preprints.org) | NOT PEER-REVIEWED | Posted: 2 October 2018 doi:10.20944/preprints201810.0025.v1

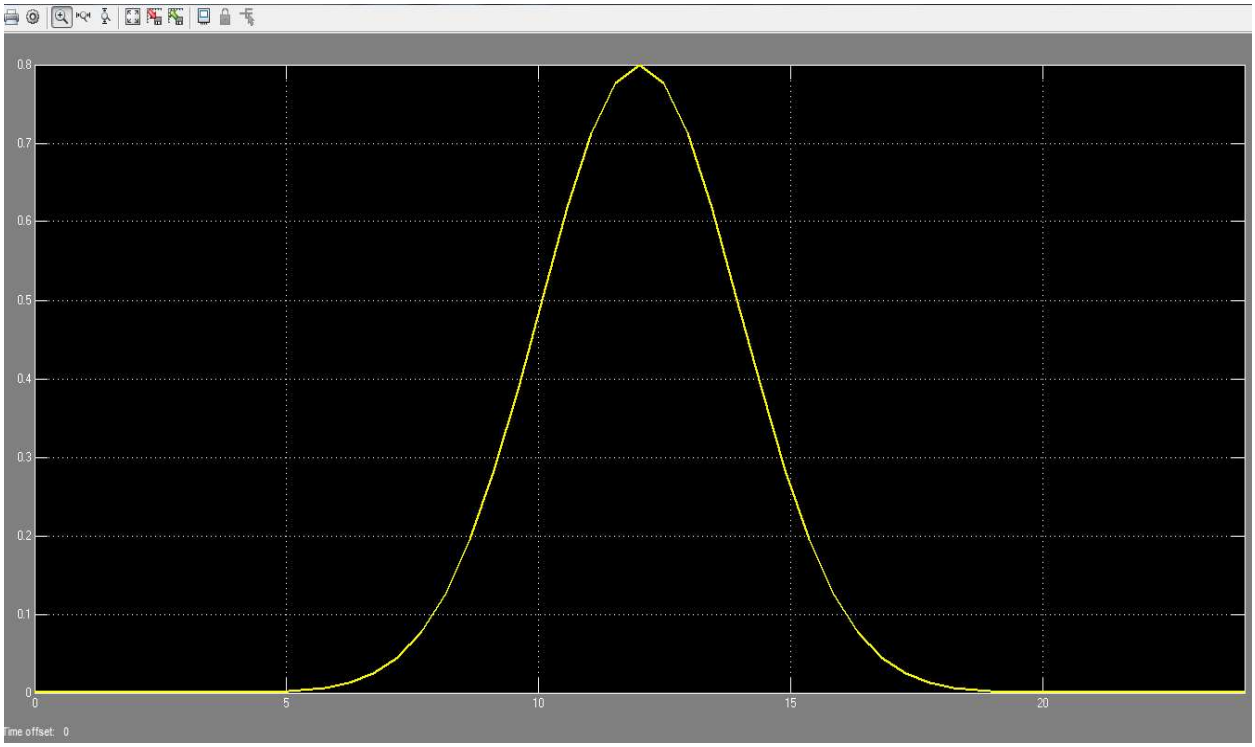


Figure 2.9: Insolation input signal generated by the model indicated in figure 2 .9 (The same the one indicated in figure 2.7)

## 2.5 Inverter Modeling

### 2.5.1 Inverter in General

DC to AC converters is known as inverters. The function of an inverter is to change DC input voltage to a symmetrical AC output voltage of desired magnitude and frequency. The output voltage could be fixed or variable at a fixed or variable frequency. Variable output voltage can be obtained by varying the input DC voltage and maintaining the gain of the inverter constant. On the other hand, if the DC input voltage is fixed, and it is not controllable, a variable output voltage can be obtained by varying the gain of the inverter. The inverter gain may be defined as the ratio of the AC output voltage to the DC input voltage [39].

The output voltage wave forms of the inverters should be sinusoidal. However, the outputs of wave forms of practical inverters are non-sinusoidal and contain certain harmonics. For low and medium power applications square wave or quasi square wave voltages may be acceptable; and for high power applications, low distorted sinusoidal wave forms are required. With the availability of high

Preprints (www.preprints.org) | NOT PEER-REVIEWED | Posted: 2 October 2018 doi:10.20944/preprints201810.0025.v1

speed power semiconductor devices, the harmonic content of output voltage can be minimized or reduced significantly by switching techniques [39].

An inverter is called a voltage fed inverter (VFI) if the input voltage remains constant, a current fed inverter (CFI) if the input current is maintained constant and a variable DC linked inverter if the input voltage is controllable.

The internal design of currently existed commercial inverters uses two techniques. The first approach is boosting the lower DC to the required higher DC then inverting; the second approach is just inverting the DC voltage level directly and then step upping the inverted AC signal to the required level. In this thesis work the second approaches is followed and MATLAB/Simulink model is indicated in figure 3.10.

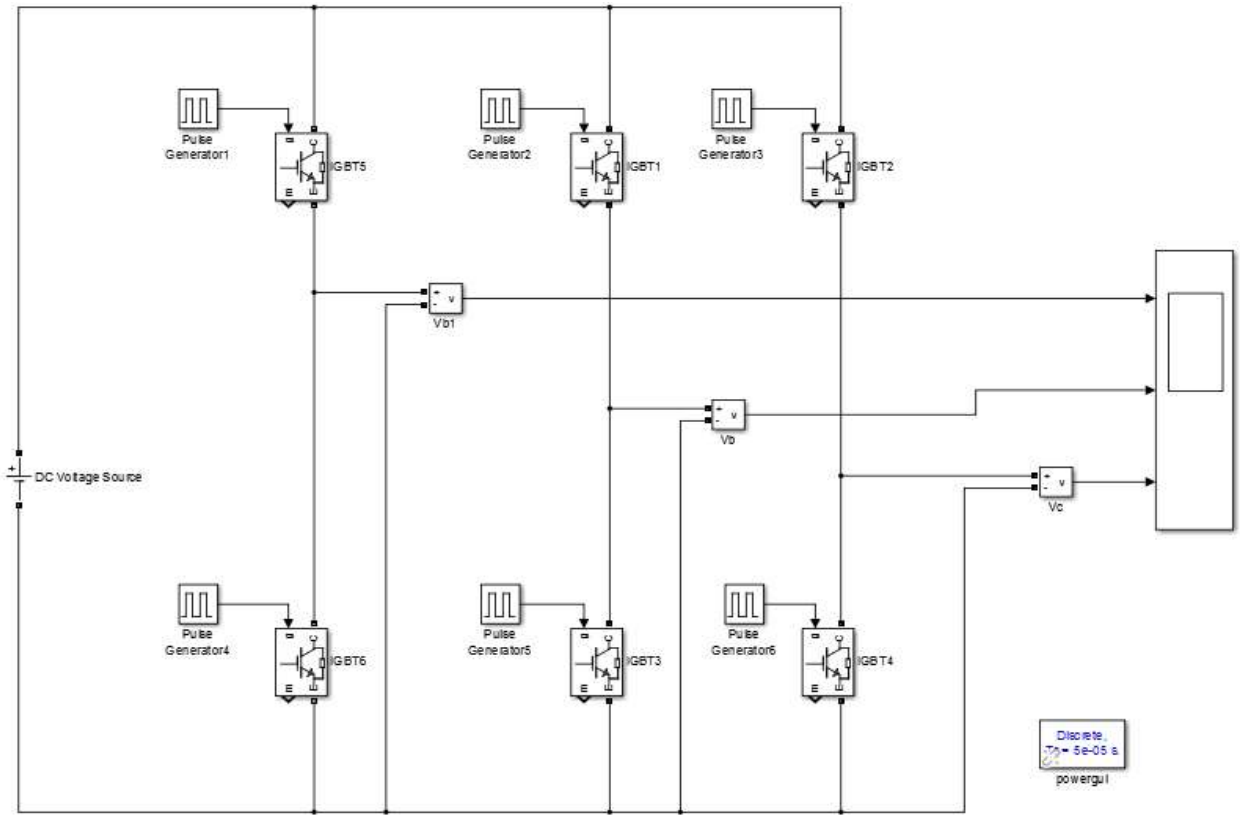


Figure 2.10: Inverter models in MATLAB/Simulink

## 2.6. Micro hydro system designing and sizing

The design parameters of micro-hydro are H=10m, assume head loss =10%,h=10-10%=9.9m, designed flow rate is 0.163$m^3$/s.

Preprints (www.preprints.org) | NOT PEER-REVIEWED | Posted: 2 October 2018 doi:10.20944/preprints201810.0025.v1

In designing the hybrid power system 35% (25.06) of the power demand of the village is covered by hydro, and to be calculated.

$$Ph = \eta gqh = 35 \quad 2.12$$

Assume loss is 10%.

$P_h$=71.6*0.35+25.06*0.1=27.6KW (The total generation capacity of the hydro system).

## 2.6.1. Hydro power subsystem model

To determine the hydropower output of a particular site requires two key parameters. These are the stream flow rate and head or vertical distance that the water drops. And the magnitude of the hydropower delivered depends mainly on the flow rate and head. The theoretical power output is expressed the equation below.

$$Ptheo = YQhg \quad 2.13$$

Where,Y=ρg, $P_{theo}$=theoretical power(w),ρ=density of water(Kg/$m^3$), Q=flow rate ($m^3$/s)

and hg = gross head (m)

**Effective head ($h_{ef}$)**

When water flows from the upper elevation to the lower one through medium channels and pipes, there is loss of energy as fractional drag and turbulence. As a result the gross head ($h_g$) will be higher than the net head or effective head ($h_{ef}$) and the effective Head ($h_{ef}$) is the difference between the gross head ($h_g$) and the head loss ($h_{loss}$).

$h_{ef} = h_g - h_{loss}$

**System efficiency (η)**

The efficiency of the micro hydropower system is the combination the turbine efficiency $\eta_t$ or water wheel and generator efficiency $\eta_g$.

$\boldsymbol{\eta=\eta_g*\eta_t}$

Then the realistic output power is estimated as

$$\boldsymbol{P}=\boldsymbol{\eta}\mathrm{Y}\boldsymbol{Qd}\mathrm{es}\boldsymbol{h}\mathrm{ef} \quad 2.14$$

Where, Qdes.is the micro hydro power designed flow rate which is 0.163$m^3$/sec (As calculated from eq 3.14).

Available from Kelta River micro hydro power generation is 13.6 kW.

Preprints (www.preprints.org) | NOT PEER-REVIEWED | Posted: 2 October 2018 doi:10.20944/preprints201810.0025.v1

### 2.6.2 Modelling of Controller

Here the PID controller is used as the controller. The error in speed is fed as input to the controller and PID controller attempts to reduce the difference between the actual speed and the reference speed by adjusting the constants of the controller. The name derives from three functions involved in calculating the corrections and is accordingly sometimes called three term control: *P* stands for proportional, *I* stand for integrator and *D* stands for derivative [40] controls. These values can be interpreted in terms of time: *P* depends on the *present* error, *I* on the accumulation of past errors, and *D* is a prediction of future errors, based on current rate of change. The output signal of the PID controller can be written in terms of the error signal as Equation 2.15

$$\theta(t) = kpe(t) + ki\int e(t)dt + kd\frac{d\theta(t)}{dt} \qquad 2.15$$

Taking Laplace transform on both sides of the Equation 4.19, we have

$$\theta(s) = kpE(s) + ki\frac{E(s)}{s} + kdsE(s) \qquad 2.16$$

The transfer function of the PID controller is

$$C(s) = \frac{E(s)}{q(s)} = kp + \frac{ki}{s} + k_d s \qquad 2.17$$

Where, $\theta(s)$ *is* the output of the PID controller represents position signal

Preprints (www.preprints.org) | NOT PEER-REVIEWED | Posted: 2 October 2018 doi:10.20944/preprints201810.0025.v1

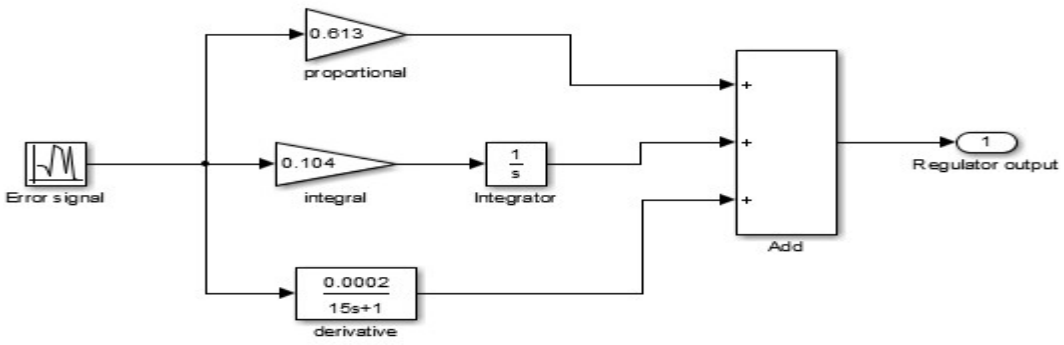


Figure 2.11: Simulink Model of a Controller

### 2.6.3 Modelling of Electro Hydro Servo System

In the model of hydro turbine governor servo motor is used to control the gate valve according to the signal of the controller. The controller nullifies the error in speed signal by sending a signal to the servo motor to control the valve.

The torque of the motor is the function of speed and error signal.

$$T_m=f(\theta, e) \quad 2.18$$

$$T_m=k_e(t) -f\theta(t) \quad 2.19$$

Where $k=\frac{dTm}{de}$ and $f=\frac{dTm}{d\theta}$

We know the mechanical relations for the motor is,

$$T_m=J\theta'' + B\theta' \quad 2.20$$

Where, *J* and *B* are friction coefficient and moment of inertia respectively.

From Equations 23and 24 above [45] we can write,

$$k_e(t) -f\theta'(t)=J\theta'' +B\theta' \quad 2.22$$

Taking Laplace transform on both sides, we have

$$\frac{\theta(s)}{E(s)} = \frac{k}{Js2+(B+f)s} = \frac{k}{s(Js+B+f)} = \frac{k}{s(tas+1)} \quad 2.23$$

Preprints (www.preprints.org) | NOT PEER-REVIEWED | Posted: 2 October 2018 doi:10.20944/preprints201810.0025.v1

Where ka=$\frac{k}{B+f}$ and $t_a$=$\frac{J}{B+f}$are gain and time constant respectively.

Here, servo motor controls the gate opening position according to change in speed at shaft of the generator to maintain the constant speed/frequency. Here, the change in speed of the generator acts as the control signal. Equation [38] is the required transfer function to develop the complete block diagram [41] of the hydro-electric servo system (Figure 2.12).

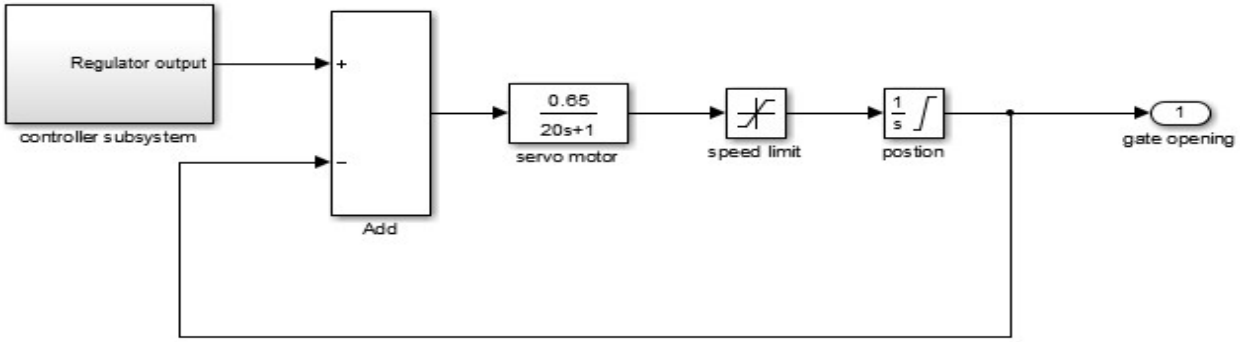


Figure 2.12: model of Hydro-Electric Servo System

## 2.6.4 Modelling of Hydraulic Turbine

This section deals with the equations describing variation in flow and developed mechanical power with respect to the turbine speed, gate opening and runner blade movement of hydro turbine. Francis is used in range of application in the hydraulic industry because it performs its operation at highest efficiency comparatively other. So that Francis turbine is used in this modelling hence the pressure of the fluid will decrease during the passage of water flow through the turbine [42]. The output power of turbine is reduced due to fall of pressure across the turbine. As the developed power in the turbine varies with the flow rate, so the system operates or gains the steady state when the flow through the penstock gets constant. The equations related to the transient performance of the hydraulic turbines are based on the following assumption [43].

- The hydraulic turbine`s blade is considered as smooth i.e. its frictional resistance is neglected.
- The water hammer on penstock is neglected.
- The fluid is considered as incompressible.

Preprints (www.preprints.org) | NOT PEER-REVIEWED | Posted: 2 October 2018 doi:10.20944/preprints201810.0025.v1

- The velocity of water in penstock varies directly with gate opening.
- The developed output power of turbine is proportional to the product of head and velocity of flow.

Equation 24 and 25 [43] represents the flow rate and the developed mechanical power at the shaft respectively in terms gate opening of the system and the net head.

$$Q = G\sqrt{H} \qquad 2.24$$

Where $Q$ is Flow rate in $m^3$/sec, $G$ is gate opening in rad,

$H$ is net head in meter. The developed power, $Pm$ in turbine can be written as

$$P_m = A_t H(Q - Q_{nl}) \qquad 2.25$$

Where, $A_t$=turbine gain, $A_t = \frac{1}{gfl - gnl} Q_{nl}$ is the no load flow rate

gfl and gnl are the full load and no load gate opening.

Equation 3.25 is modified to describe the motion of the water in penstock by Equation 2.25.

$$U = KuG\sqrt{H} \qquad 2.23$$

Where, $U$ is the velocity of the water in penstock and $K_u$ is a proportional constant.

Once the velocity of the water in penstock is determined, the relation of flow rate, head could be established 3.23 and 3.24.

$$Q = Au \qquad 2.24$$

The acceleration of the fluid in the penstock is described by Equation 26 [37]

$$\frac{du}{dt} = -\frac{\alpha g}{L}(H - Ho) \qquad 2.25$$

Where α is the acceleration due gravity, L is the length of penstock.

The mechanical power output is given by

$$P_m = P - P_L \qquad 2.26$$

Where, $P_l$ is the fixed power loss in turbine due to friction.

Preprints (www.preprints.org) | NOT PEER-REVIEWED | Posted: 2 October 2018 doi:10.20944/preprints201810.0025.v1

$$P_L=U_{NL}H \qquad 2.27$$

Where, $U_{NL}$ stands for no load speed.

The hydraulic characteristics and mechanical power output of the turbine is modelled here. The nonlinear characteristics of hydraulic turbine are neglected in this model. The complete hydro turbine model is shown in Figure 3.13. The actuator's (hydro-electric servo motor) output is the gate opening and it controls the valve to maintain a uniform speed by regulating the rate of water flow. The transfer function represented by Equation relates the flow rate $Q$ and net head $H$. Here ($H$-$H_0$) is entered as an input and the flow rate is the output signal of the transfer function. $H_0$has been assumed a static head with reference value of 1pu.

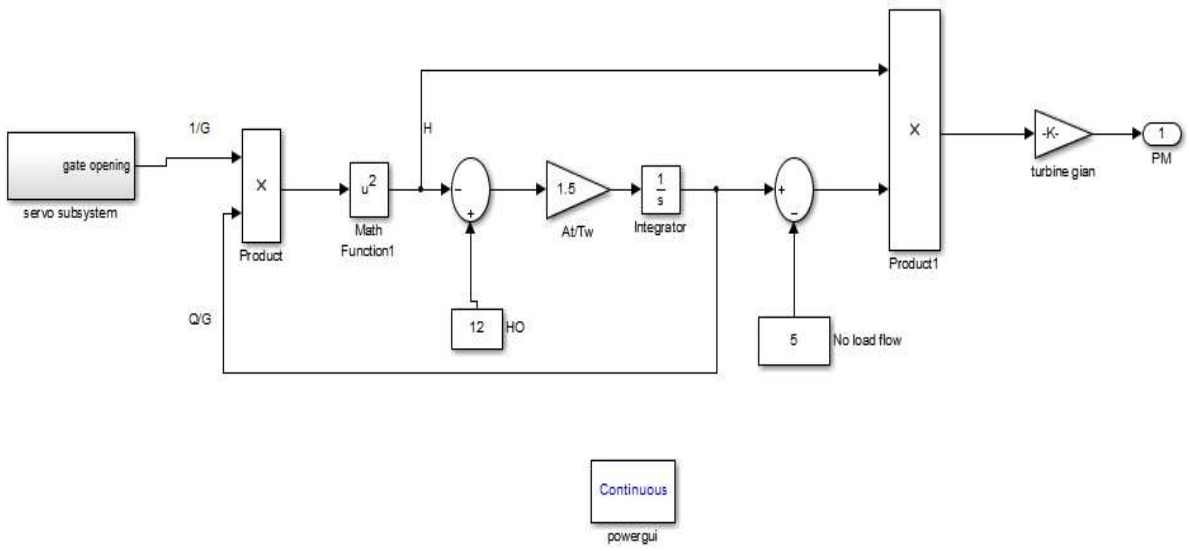


Figure 2.13: MATLAB/Simulink Model of Hydro Turbine

## 2.6.5 MATLAB/Simulink Model of Hydro Turbine Governor

Hydro turbine governor is a major part of hydro power plant. It is basically used for two purposes - firstly, it develops mechanical power at the shaft of the generator which is fed to the generator for production of electricity. And secondly, it controls the variation of speed of the generator such that the generated frequency remains constant. The PID controller, hydroelectric servo system and hydraulic turbine are the main components of the hydro turbine governor. The mathematical modelling and block formation has been done in the previous section of this chapter. These block model of components are connected in such a manner that the generated frequency remains

Preprints (www.preprints.org) | NOT PEER-REVIEWED | Posted: 2 October 2018 doi:10.20944/preprints201810.0025.v1

constant. The block diagram of hydro turbine governor is shown in Figure 2.14. The first element of the governor is PID controller. The error in speed and deviation of power is entered as input to the controller, which generate the position signal at the input of the hydro-electric servo motor. Further the servo motor response by controlling the valve according to input signal to the servo mechanism. The valve is used to control the flow rate such that the generated frequency of the system remains constant.

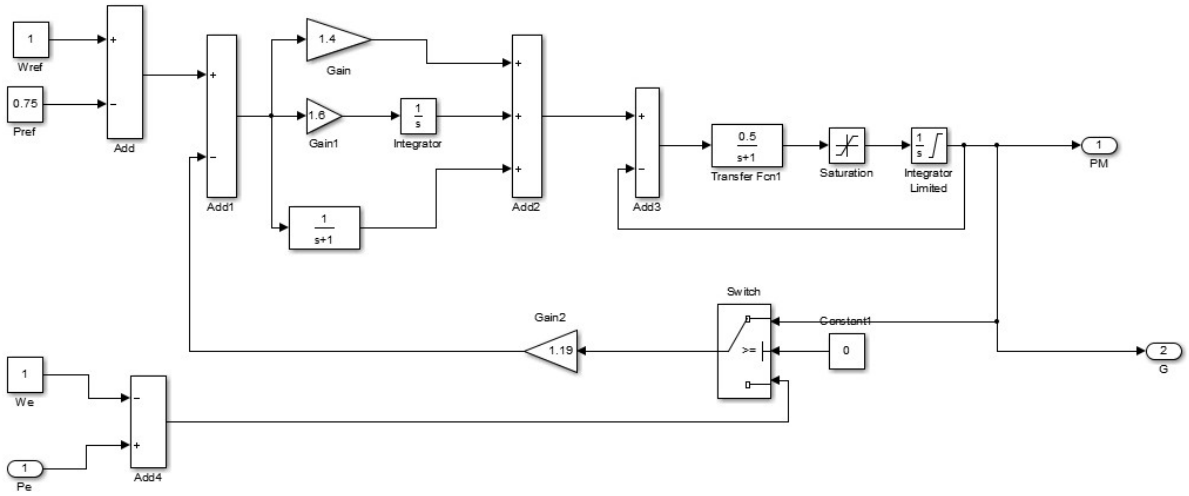


Figure 2.14: MATLAB/SimulinkModel of Hydro Turbine Governor

The mathematical model of a synchronous machine uses Park's equations for the electrical dynamics [44]. Equations 3.15 to 3.27 are here used to model the electrical dynamics of the synchronous generator [44].

$$T''do\frac{dE''q}{dt} = E'q - E''q + (X'd - X''d)Id \qquad 2.28$$

$$T''qo\frac{dE''d}{dt} = E'd - E''d + (X'q - X''q)Iq \qquad 2.29$$

$$T'do\frac{dE'q}{dt} = E'f - E'q + (Xd - X'd)Id \qquad 2.30$$

$$T'qo\frac{dE'q}{dt} = E'd - E''q + (Xq - X'q)Iq \qquad 2.31$$

Preprints (www.preprints.org) | NOT PEER-REVIEWED | Posted: 2 October 2018 doi:10.20944/preprints201810.0025.v1

On the basis of these generalized equations, the synchronous machine model is simulated in MATLAB/Simulink software. This model is available as a single block (Figure 2.15) with various terminals in MATLAB/Simulink library. The model takes into account the dynamics of the stator, field, and damper windings.

The individual sub-models like hydro turbine governor, synchronous generator, excitation system and 3-phase RLC load are now connected together to form the complete block diagram of micro hydro power plant (Figure 2.15)

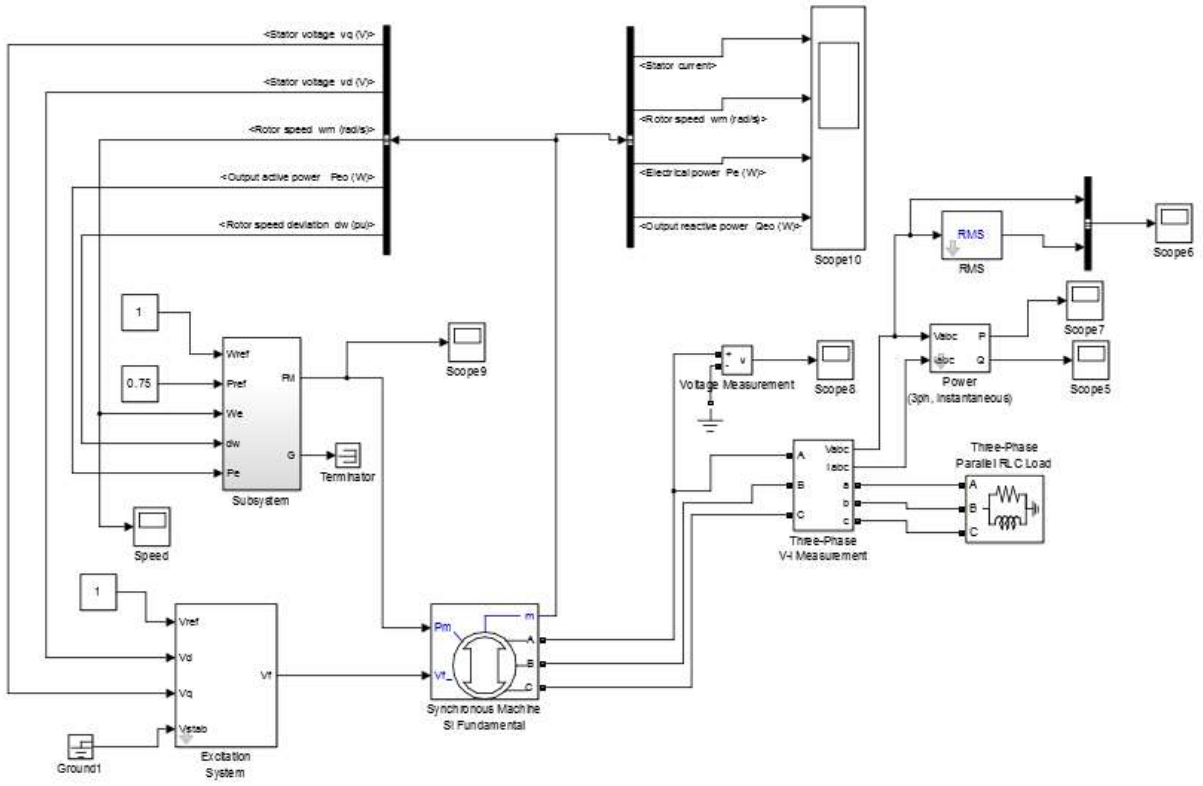


Figure 2.15: MATLAB/Simulink Model of a Hydro Power

## 2.7. Proposed model using fuzzy logic controller for the hybrid system

The proposed hybrid system consist solar, micro-hydro and wind renewable energies. The capacity of electric generation in hybrid system is to satisfy the power demand on the atmospheric conditions. Fuzzy logic controller is used to control the power efficiently and to serve the power demand of the costumer.

The controller looks first at the load and switches the appropriate sources to meet the demand from the costumer side. Thus there is no need of battery and charge controller.

Preprints (www.preprints.org) | NOT PEER-REVIEWED | Posted: 2 October 2018 doi:10.20944/preprints201810.0025.v1

Basically comprehensive controller is essential to efficiently manage the energy balance between the total generation and the total demand. The important requirements of the standalone hybrid system are the availability of renewable energy resources, and the combination has formulated.

### *2.7.1. Fuzzy* Logic Controller algorithm

Fuzzy logic controller is an intelligent tool to manage the integrated energy sources in such a way that it meets the load requirement under varying load conditions. The procedures in making the controller designs are setting the constraints, assigning the linguistic variables and setting the rules for the controller. In this thesis work the Fuzzy Logic Controller has four inputs and one output. The input linguistic variables of FLC are Solar power (Sp), Micro-hydro power (Hp), wind power (Wp) and Power demand (PD) and the single Output linguistic variable is out power (Po). Each input linguistic variable has three linguistic values called Low, Medium and Large and the output linguistic variable has Wp only, Wp+Sp, Hp+Wp, Hp+Sp+Wp linguistic values. Triangular membership function for Justification, Mamdani inference system for rule processing and center of gravity for De-fuzzy analysis and process by fuzzy logic is used. A typical fuzzy system consists of a membership functions, rule base, inference procedure and rule viewer which were explained in the following sections. After giving membership function for each input output linguistic values and generating the possible operational rules then the next step is to evaluate the rules of the controller for the input values if the output is appropriate or not. To see the overall performance the hybrid system, components are assumed to produce random signal.

**A) Fuzzy interface model**

Preprints (www.preprints.org) | NOT PEER-REVIEWED | Posted: 2 October 2018 doi:10.20944/preprints201810.0025.v1

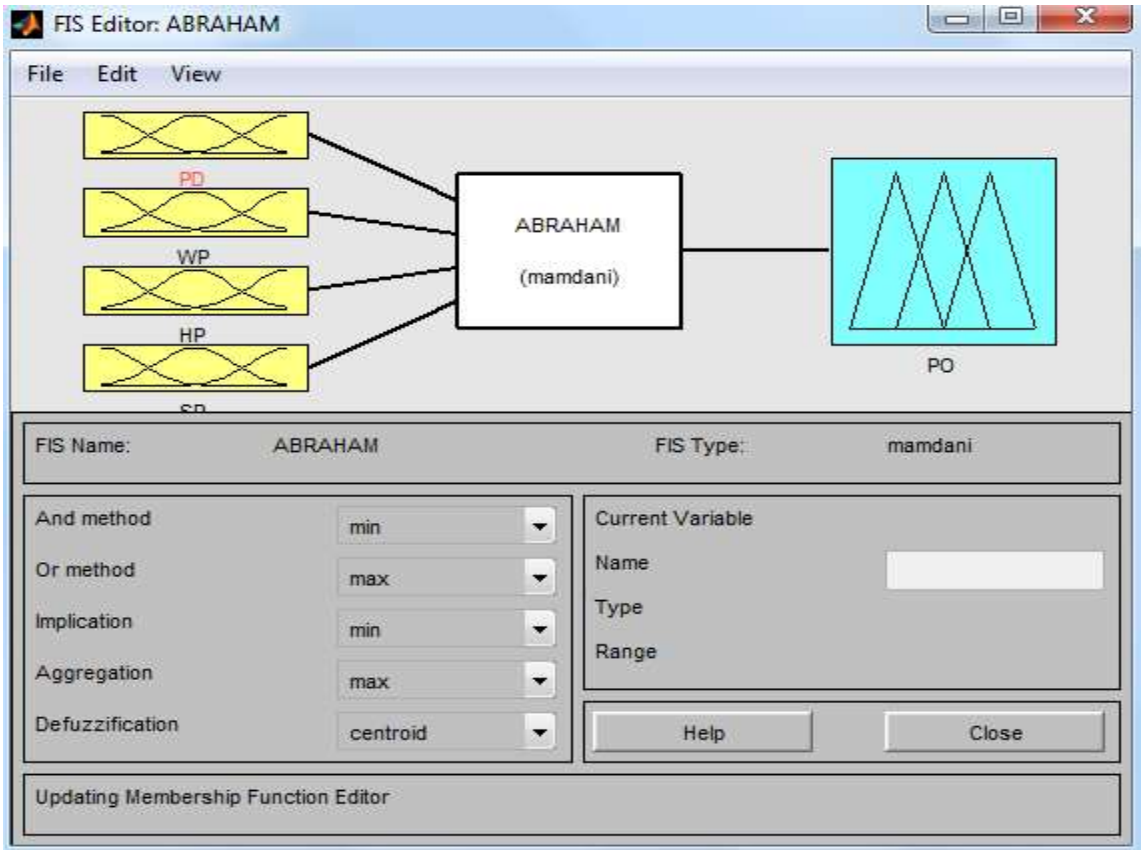


Figure 2.16: Fuzzy interface model

**B) Membership function of power demand (PD)**

The power demand (PD) is one of the input linguistic variables having three linguistic values, Low (0 15 30), Medium (20 35 50) and Large (35 53.3 71.6).

Preprints (www.preprints.org) | NOT PEER-REVIEWED | Posted: 2 October 2018 doi:10.20944/preprints201810.0025.v1

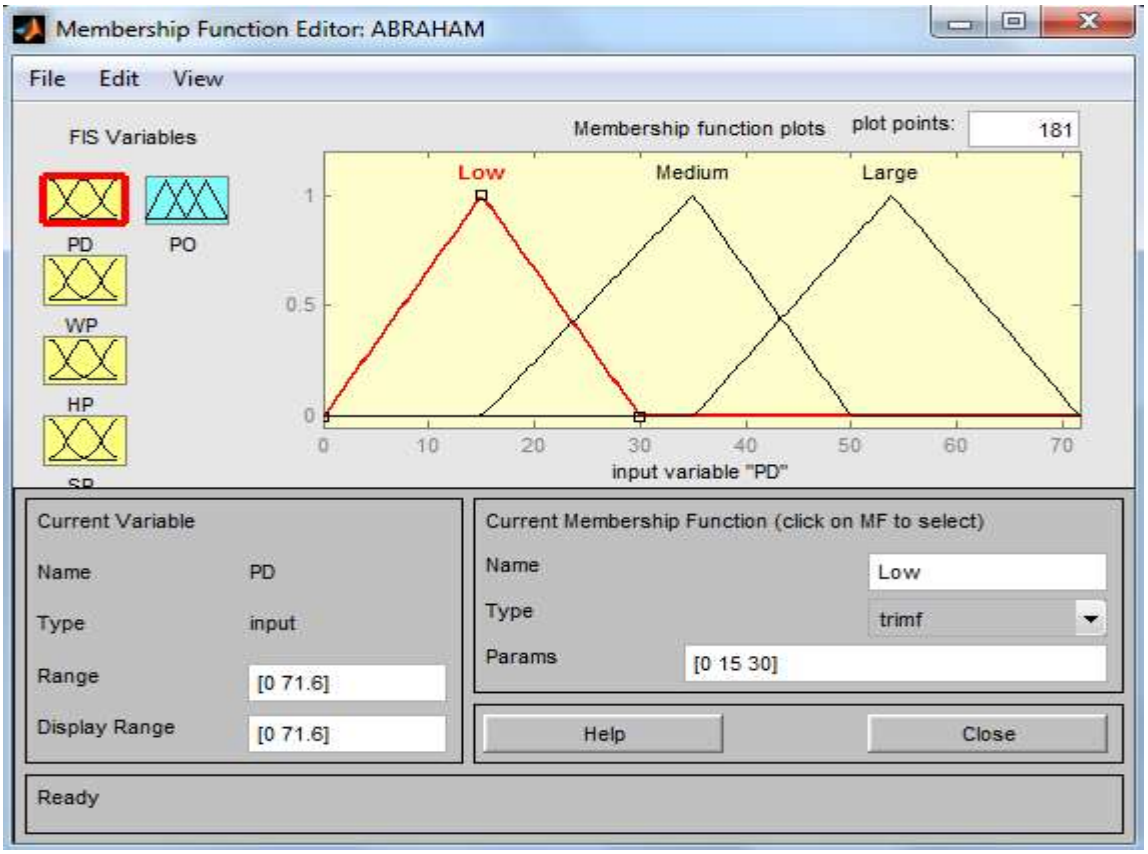


Figure 2.17: Membership function of power demand

**C) Membership function of wind power (Wp)**

Wind power is the fourth input linguistic variables having three linguistic values, Low (0 7.5 15), Medium (10 18.5 27), Large (25 32.95 40.9).

Preprints (www.preprints.org) | NOT PEER-REVIEWED | Posted: 2 October 2018 doi:10.20944/preprints201810.0025.v1

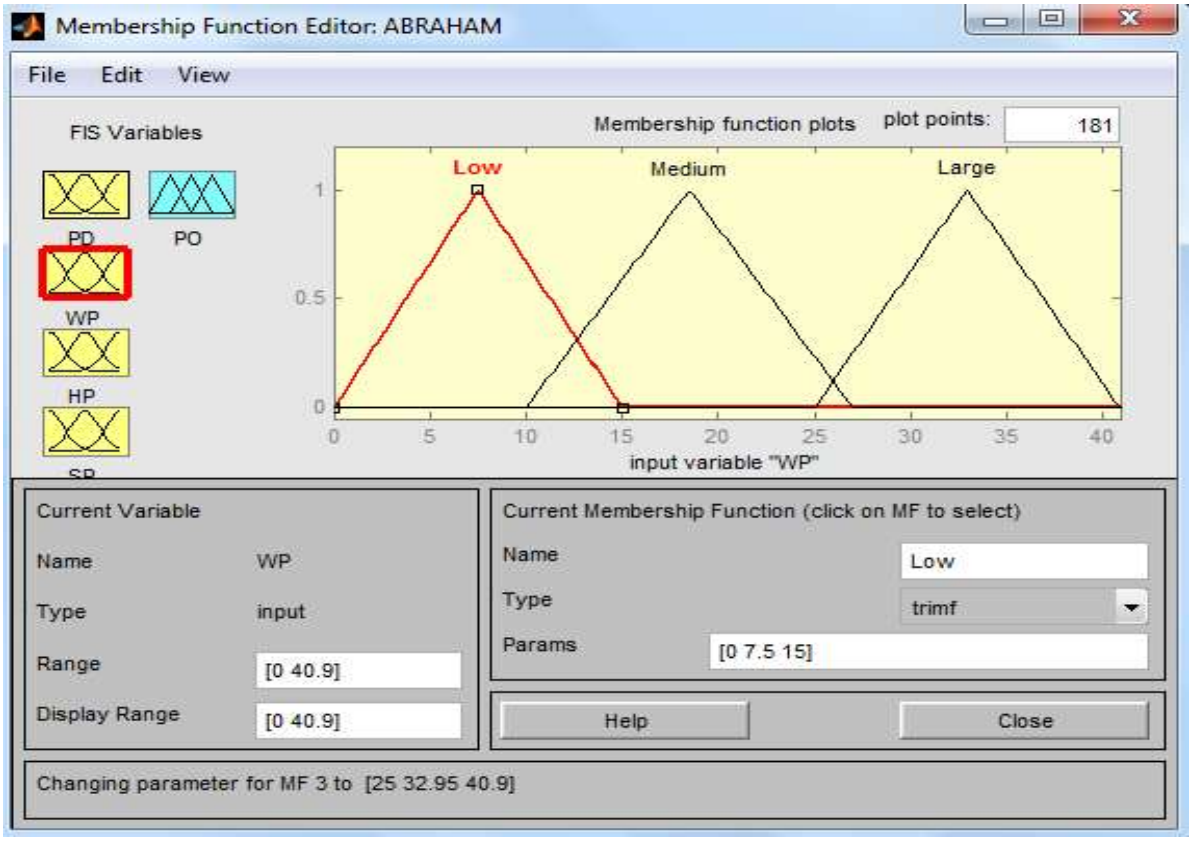


Figure 2.18: Membership function of wind power

**D) Membership function of Micro-hydro (Hp)**

Micro-hydro is the second input linguistic variables having three linguistic values, Low (0 5 10), Medium (5 11.5 18), Large (15 21.3 27.6).

Preprints (www.preprints.org) | NOT PEER-REVIEWED | Posted: 2 October 2018 doi:10.20944/preprints201810.0025.v1

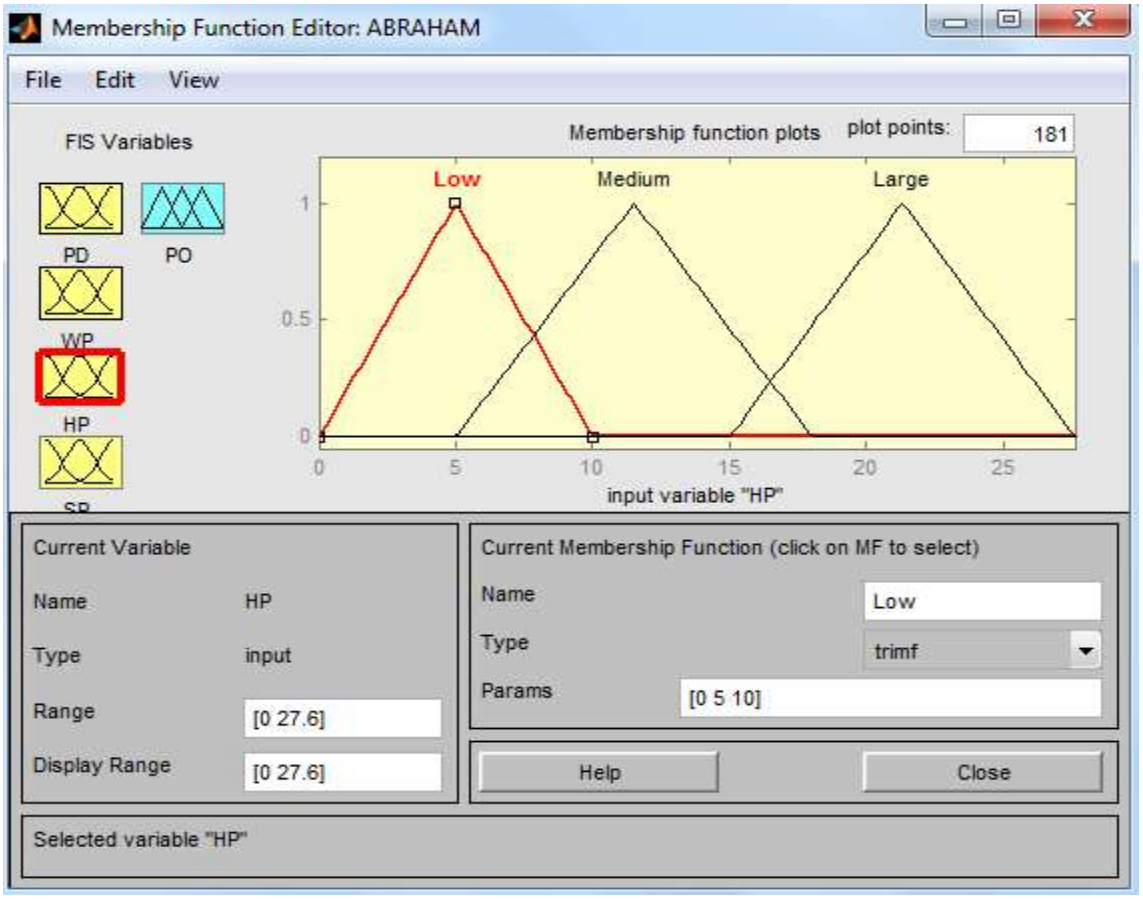


Figure 2.19: Membership function of micro-hydro power

**E) Membership function of solar power (SP)**

Solar power is the third input linguistic variables having three linguistic values, Low (0 2 4), Medium (3 5.5 8), Large (6 8.1 10.2).

Preprints (www.preprints.org) | NOT PEER-REVIEWED | Posted: 2 October 2018 doi:10.20944/preprints201810.0025.v1

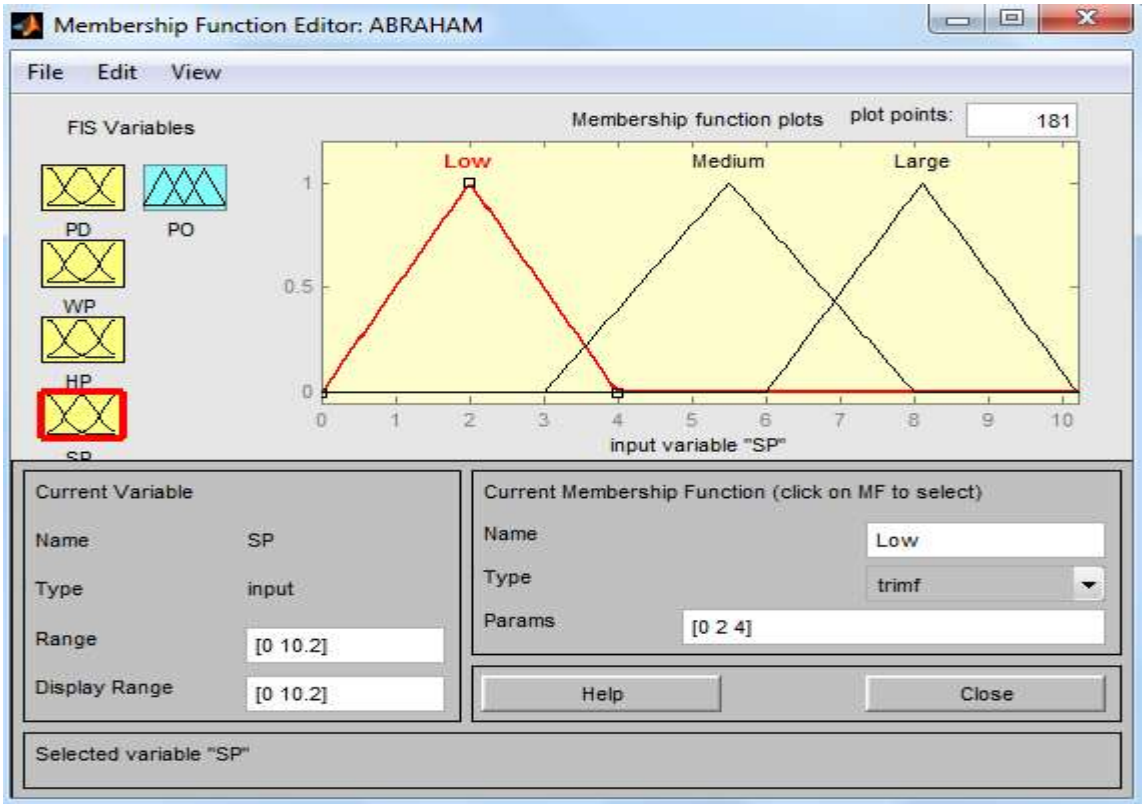


Figure 2.20: Membership function of solar power

**F) Membership function of output power (Po)**

Output power is the only output linguistic variables having three linguistic values, WP-only(0 14.5 29), Wp+Sp(20 28 36), WP+HP(30 45 60),Hp+Sp+Wp(40 55.8 71.6).

Preprints (www.preprints.org) | NOT PEER-REVIEWED | Posted: 2 October 2018 doi:10.20944/preprints201810.0025.v1

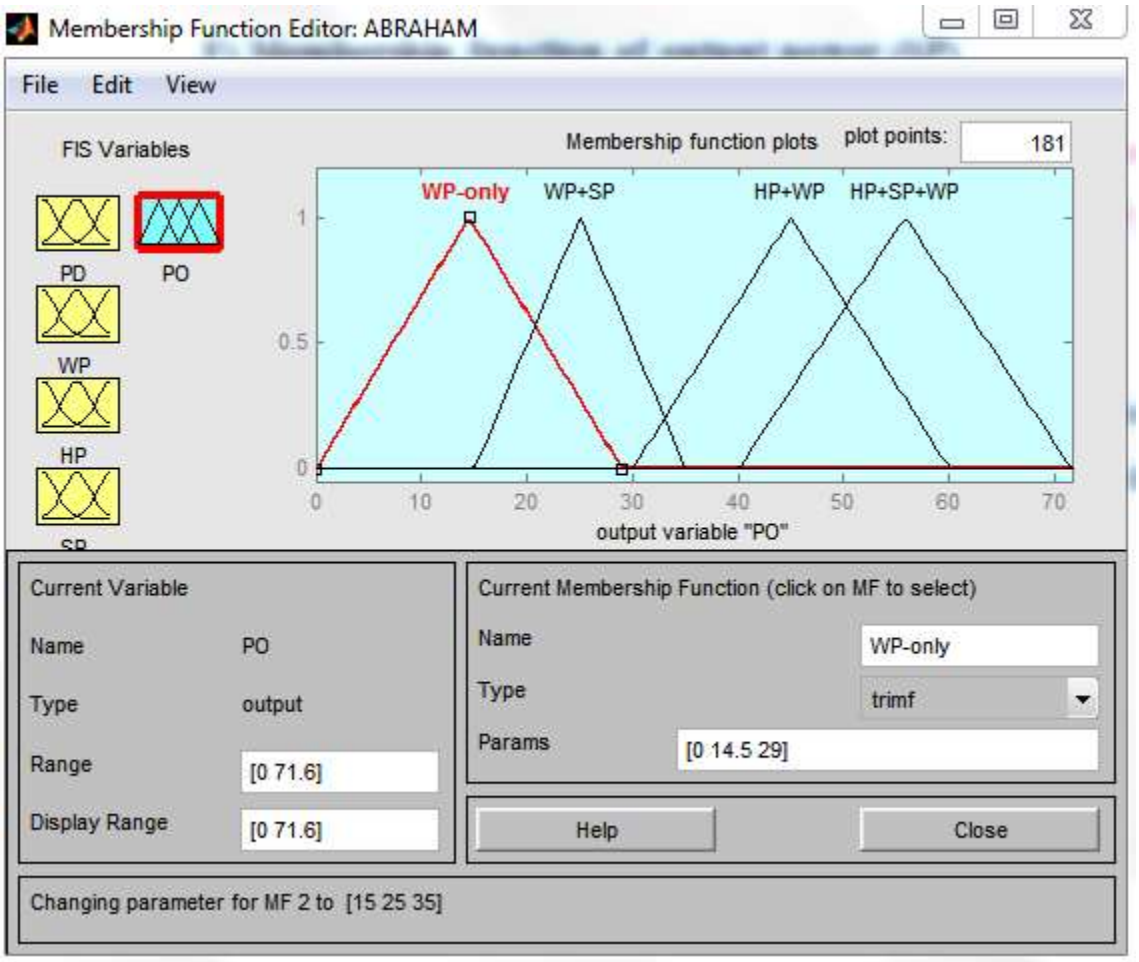


Figure 2.21: Membership function of output power

**G) Real time modeling of fuzzy logic rules**

Here is model of fuzzy logic controller having four inputs and one output. In control box, a set of rules have been written. The system was operated in accordance to the rules set.

*Preprints* (www.preprints.org) | NOT PEER-REVIEWED | Posted: 2 October 2018 doi:10.20944/preprints201810.0025.v1

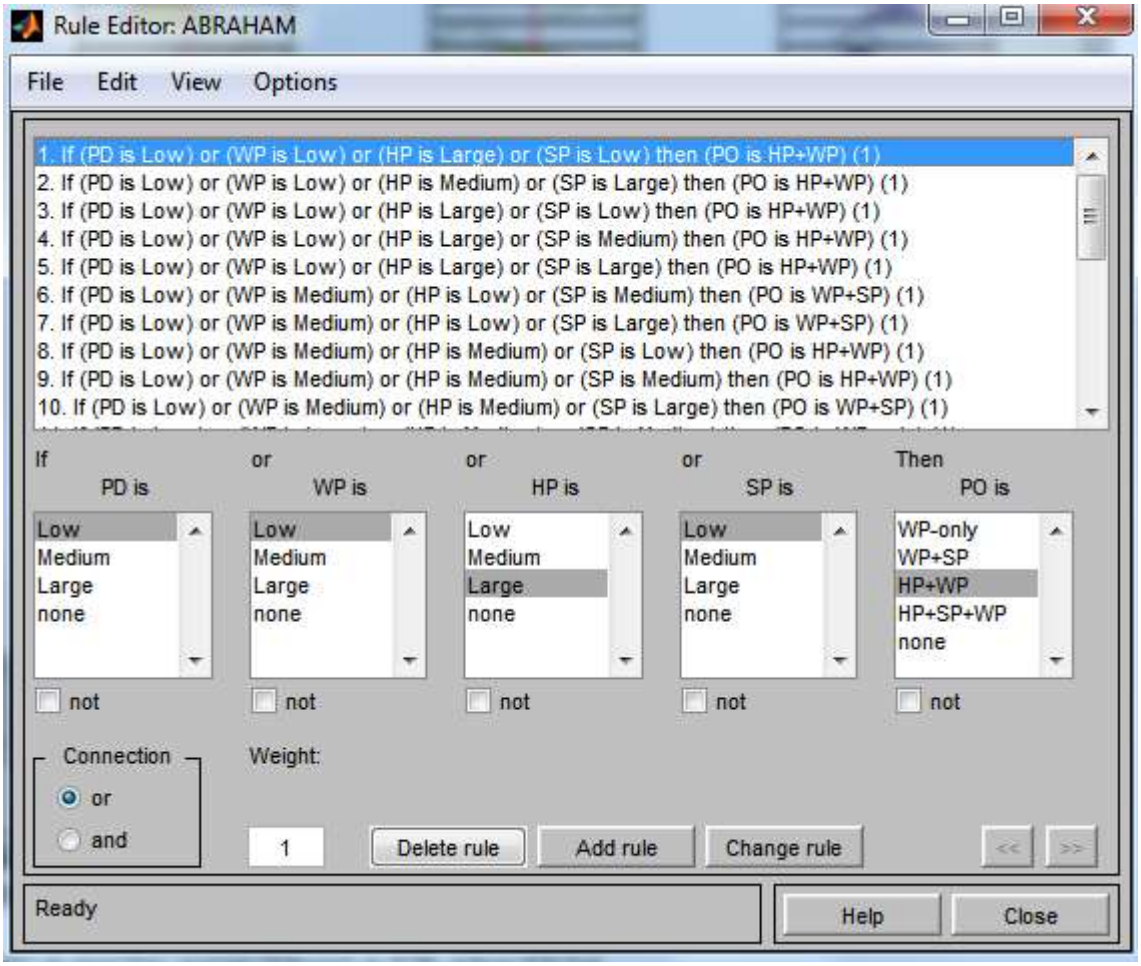

Preprints (www.preprints.org) | NOT PEER-REVIEWED | Posted: 2 October 2018 doi:10.20944/preprints201810.0025.v1

Figure 2.22: fuzzy logic controller rule editor

## 2.7.2. Rule evaluating

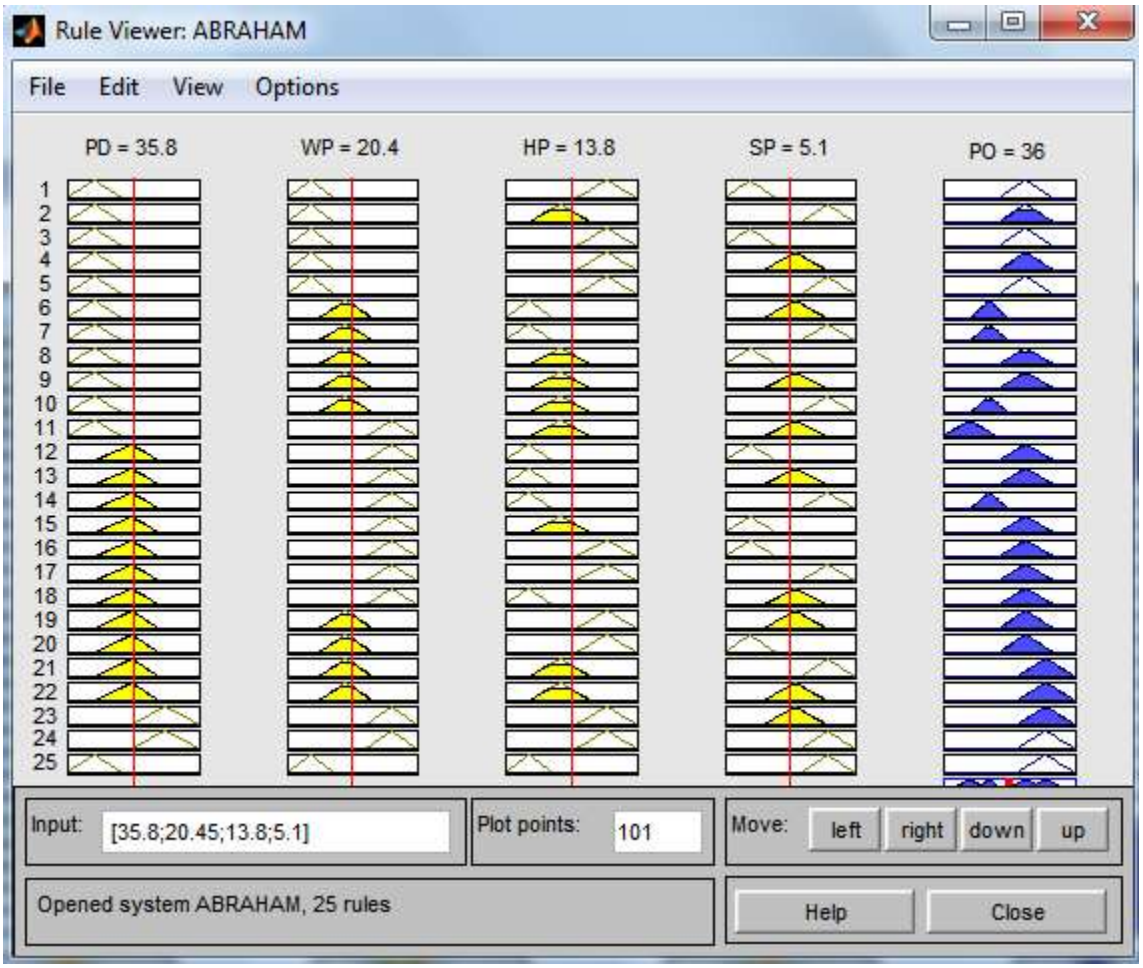


Figure 2.23: Rule viewer

## 2.7.3. Overall fuzzy logic controller system

The solar power, micro-hydro power, wind power and power demand are the input parameters of the controller. PD,HP,SP and WP indicates the demand power from the customer side, power from micro-hydro, power from solar system and power from wind power respectively. The power coming from each component power sources is assumed to be Gaussian random signal generator. The multiport conditional switch will take an action according to the rules written in fuzzy logic controller.

Preprints (www.preprints.org) | NOT PEER-REVIEWED | Posted: 2 October 2018 doi:10.20944/preprints201810.0025.v1

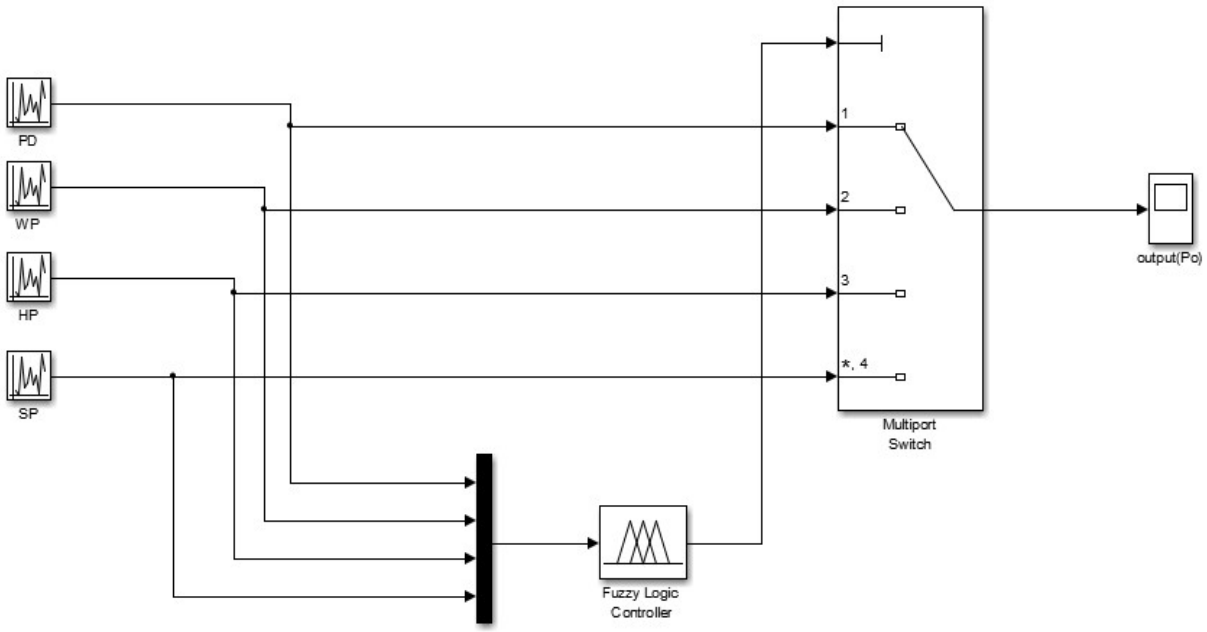


Figure 2.24: Overall hybrid system

### *2.7.3.1. Performance evaluation of the designed fuzzy logic controller*

To evaluate the designed controller, it possible to take different operating conditions, as flow.

## Case one

If the demand power PD is 16kw, WP is 11kw, HP is 8kw, and SP is 0kw then the output power of fuzzy logic controller is indicated in figure 2.25.

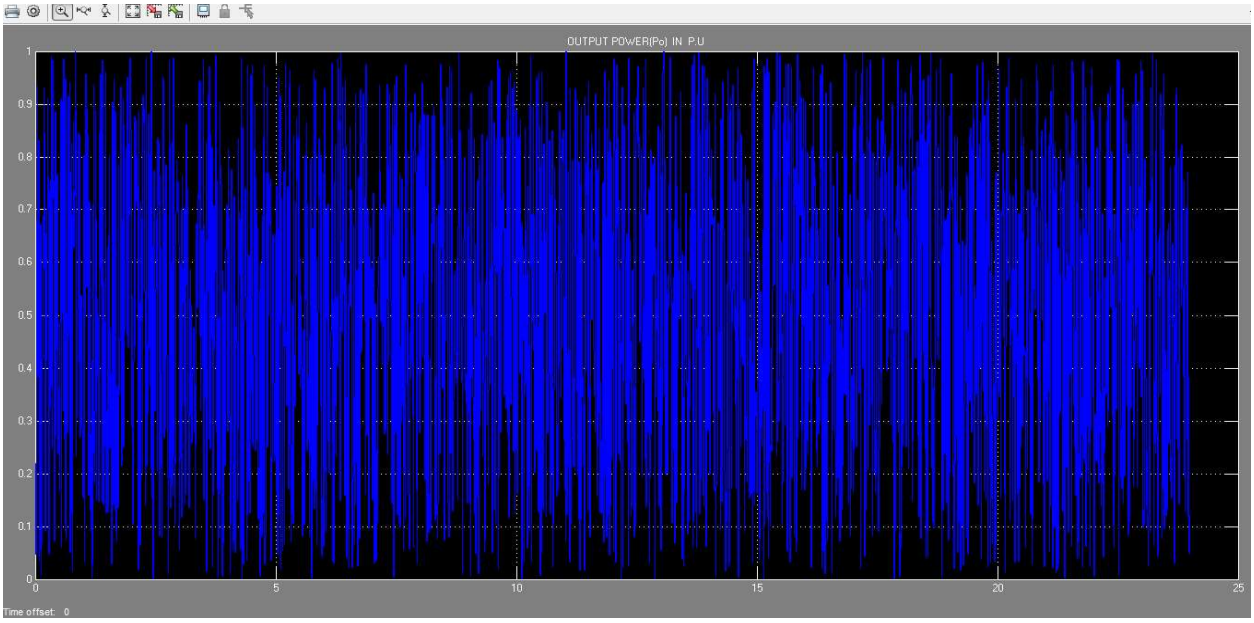

Preprints (www.preprints.org) | NOT PEER-REVIEWED | Posted: 2 October 2018 doi:10.20944/preprints201810.0025.v1

Figure 2.25: Simulation result of fuzzy logic controller in case one

If the demand power PD is 45, WP is 14kw, HP is 25kw, and SP is 9 then the output power of fuzzy logic controller is indicated in figure 2.26.

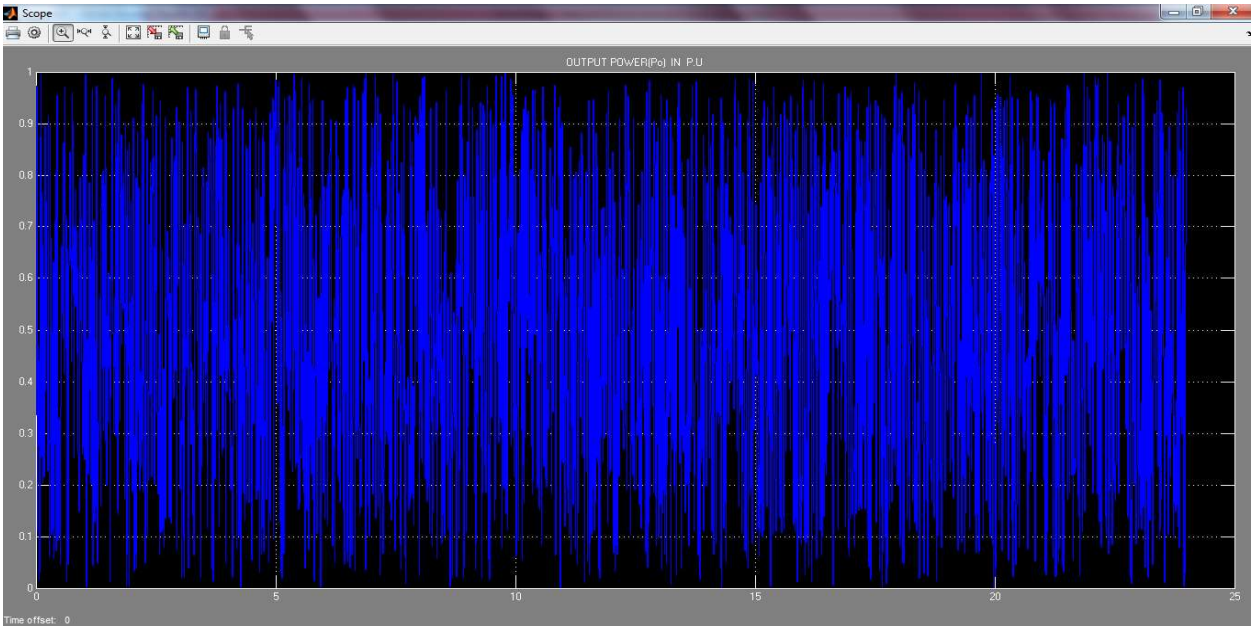


Figure 2.26: Simulation result of fuzzy logic controller in case two

## Case three

If the demand power PD is 64kw, WP is 36kw, HP is 27kw, and SP is 10kw then the output power of fuzzy logic controller is indicated in figure 2.27.

Preprints (www.preprints.org) | NOT PEER-REVIEWED | Posted: 2 October 2018 doi:10.20944/preprints201810.0025.v1

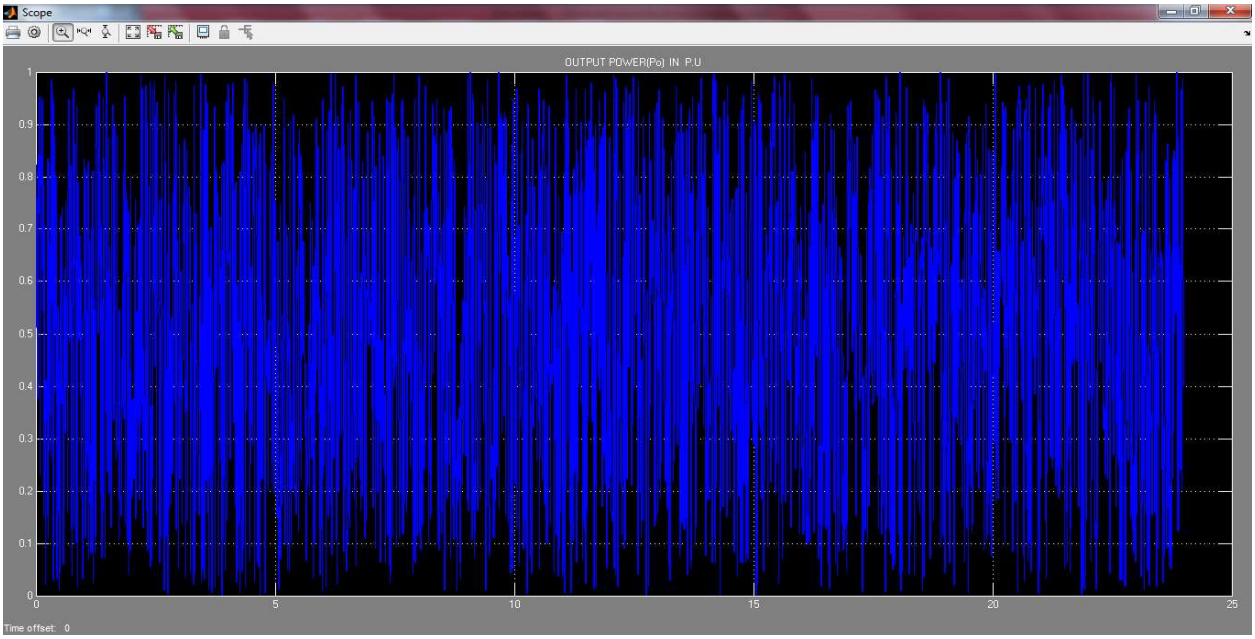


Figure 2.27: simulation result of fuzzy logic controller in case three

## 3. CONCLUSIONS

A hybrid power system which consists of hydro, PV-arrays and wind turbines with energy storing devices (battery bank) and power electronic devices has been presented to achieve an efficient and cost competitive system configuration so that hybrid power sources could improve the life of people especially in rural areas where electricity from the main grid has not reached yet.

After data collection and community load estimated, a hybrid power system containing PV, hydro and wind power units are studied. Then, with the optimized hybrid system, MATLAB/Simulink model is developed to examine the dynamic responses of the designed power system over 24 hours of typical day. Finally, grid extension from the closest substation has been designed for comparison cost against the designed hybrid power system.

The result of the dynamic responses of the dynamic model that contains the optimal hybrid system shows that the overall power management strategy is effective and the load demand is balanced successfully. Moreover, the inverter output voltage waveforms obtained from the inversion of battery bank terminal DC bus voltage also authenticate that such a hybrid system can supply electric energy to the end users with the required voltage magnitude and frequency levels.

Fuzzy logic controller is used to select the appropriate power source for the load depending on the resource available. According to the rules written on fuzzy logic control, the possible power sources can be wind energy alone, hybrid of wind and hydro, hybrid of wind and solar and hybrid

 doi:10.20944/preprints201810.0025.v1

of all. The intelligent controller is used to make intelligent decision by sensing the type and amount resource available, and then it selects appropriate alternative sources. The simulation result tells, the controller can supply the intended power demand in different cases (the output power from controller is from 5kw to 68kw to satisfy the electric demand of customer).

Finally, HOMER software is also used to compare the investment cost of the hybrid system against the cost required for extending the grid. As a result, it is found that the hybrid system is cost effective for an area which is found at a distance greater than 23.9km (which is the breakeven grid extension distance) from the existing grid found nearby. The study area is positioned below the breakeven grid extension distance (15km), current electricity tariff in the county (average 0.09 $/kWh) where the main source of electric energy is hydro-power supported by geothermal plants and recently integrated wind farms. The costs of the feasible system obtained in this study are high; the COE is 0.0.642 dollars per kilowatt hour. In this regard, grid extension is preferable for the case study area. However, considering the shortage of power in the country in general and in rural areas in particular, rapid growth of industries in urban areas, its role in the protection of vegetation and forestry and the prevention of soil degradation, the improvement to the quality of life of the many people residing in the countryside and the future situation regarding fossil fuel sources, the cost of the hybrid should not be seen as a significant impact.

 doi:10.20944/preprints201810.0025.v1

## References

[1] J.B.Gupta, power system, New delhi, 2004.

[2] Frank, Yebah, Dazie, Design of a grid connected photovoltaic system for KNUST and Economic and enviromental Analaysis of the design system available, p. 6, 2010.

[3] Dereje, Derbew Ethiopian's renewable energy power potential and development oportunities, Adiss Ababa, 2013.

[4] Agawal, Weng, Rajesh, K.Gupta and Yuvraji, micro-system dirving smart energy metering in smart grids, 2010.

[5] Bin Sun, Xuan Liu, Microgrids, *corporate research,* 2010.

[6] Laxmi Shankar, Tripathi, Study of microgrid and its communication protocol, 2011.

[7] SHIVYA, SRIVASTAVA, SMART MICROGRID, 2014.

[8] The word bank group, Technical and economic assessment of off-grig,mini-grid and grid electronics techonologies, 2006.

[10] Elhadidy Shaahid, feasibility study of the stand-alone hybrid systems,205.

[11] Guptaet, solar wind hybrid power generation system, 2006.

[12] Danish Wind Industry, Association, 2011.

[13] Dannish Wind Industry, Association, (Jan 2011), http://www.windpower.org/en/tour.

[14] Luque A,Hegedus Handbook of Photovoltaic Science and Engineering, West Sussex: John Wiley & Sons Ltd., 2003.

[15] Bizuayehu Tesfaye, Improved Sustainable Power Supply for Dagahabur and Kebridahar Town of Somalia Region in Ethiopia, 2011.

[16] Mark R, Patel, Wind and Solar Power Systems: Design, Analysis, and Operation. 2nd Ed. Boca Raton: Taylor & Francis Group, 2006.

[17] Duffie W, Solar Engineering of Thermal Processes. 3rd ed. New Jersey, John Wiley and Sons, Inc. 2006.

[18] Tzanakis I, Combining Wind and Solar Energy to Meet Demands in the Built Environment 2006.

[19] Twidell J, And Weir T, Renewable Energy Resources, 2nd Edn, London: Taylor & Francis, 2006.

[20] V.Aldo, Fundamentals of Renewable Energy processes, 2005.

[21] Mukind R, Patil, Wind and Solar Power Systems,, CRC pres LLC, USA, 1999.

[22] Etihiopia Japanes Embasy, in Study on the Energy Sector in Ethiopia,http://www.et.emb-japan.go.jp/electric_report_english.pdf, 2008.

[23] Gerlach A, Husiak M, Peter C, Adelmann P, Winiecki J, Shutzeichel H,Tegaye S, Gashie W,and Breyer Ch, Electrifying the Poor: Highly Economic Off-Grid PV Systems in Ethiopia

a basic for sustainable development http/www.arcfinance.org/pdfs/news/Ethiopia paper2009pdf.

[24] Mulugetta Y. and Drake F, Assessment of solar and wind energy in Ethiopia. I. Solar energy, vol. Vol. 57, pp. 205-217, 1996.

[25] Gtz, Policy and regulatory framework conditions for small hydro power in Sub-Saharan Africa Discussion paper, July 2010.

[26] U.S. Department of Interior. Supt. Of Documents, Design of Small Dams,Printing Office, Washington DC 20402, Washington.

[27] Science popular, Water Power for Your Home, 1977.

[28] Gipe P, Wind Power: Renewable Energy for Home, Farm, and Business,Chelsea Green Publishing Company, 2004.

[29] Science popular, Water Power for Your Home, 1978.

[30] Ackermann T, Wind Power in Power Systems. Chichester, 2005.

[31] Pirker O, Role of storage and pump storage hydro power plants for grid regulation.2nd Eur electric Small Islands Seminar, Ajaccio, 2008.

[32] Mathew S, wind energy: fundamentals, Resource Analysis and Economics, Berlin, 2006.

[33] Patel M, Wind and Solar Power Systems: Design, Analysis, and Operation. 2nd Ed, Taylor & Francis Group.

[34] All Small Wind Turbines website: http://www.allsmallwindturbines.com/, [Online].

[35] The Micropower Optimization Software, Ver. 2.68 beta, http://homerenergy.com/.

[36] Tsai H, 2008, Development of Generalized Photovoltaic Model Using Matlab/Simulink, Proceedings of the World Congress on Engineering and Computer Science (WCECS), San Francisco, USA.

[37] Rashid M, 2004, Power Electronics Circuits, Devices and Applications, 3rd edition, Pearson Prentice Hall, ISBN: 0-13-122815-3.

 doi:10.20944/preprints201810.0025.v1

[38] Becherif M, Paire D, Miraoui A, 2007, Energy Management of Solar Panel and Battery System with Passive Control, International Conference on Clean Electrical Power, pp. 14-19.

[39] http://wwwdsa.uqac.ca/~rbeguena/Systemes_Asservis/PID.pdf

[40] Zhang X,Zhang M, An adaptive fuzzy PID control of hydro-turbine governor, International Conference on Publication Year: 2008, 4139 – 4143(2002).

[41] Hesmondhalgh E and Laithwaite R, Method of analysing the properties of 2-phase servo-motors and AC tachometers, Volume 70, 1987-1993.

[42] Kaabeche A, Belhamel M and Ibtiouen R, Optimal sizing method for stand-alone hybrid PV/wind power generation system, Revue des Energies Renouvelables SMEE'10 BouIsmail Tipaza, 205 – 213 (2010).

[43] Singh G and Chauhan et al.,Simulation and modeling of hydro power plant to study time response during different gate states, International Journal of Advanced EngineeringSciences and Technologies, Volume 10 (1), 042 – 047 (2011).